



INSTITUTO SUPERIOR TÉCNICO
Universidade Técnica de Lisboa

Numerical simulation of the seismic behavior of steel storage pallet racking systems

Gonçalo Eurico Novais Ribeiro Coutinho

Dissertação para a obtenção do Grau de Mestre em

Engenharia Civil

Júri

Presidente: Professor José Câmara

Orientador: Professor Luís Calado

Co-Orientador: Professor Carlo Castiglioni

Vogal: Professor Jorge Proença

Outubro 2008

ACKNOWLEDGEMENTS

Special recognition and extend thanks to Professor Carlo Castiglioni, Full Professor, from Politecnico di Milano, to Professor Luis Calado from Instituto Superior Técnico, Lisbon and to Dr. Graham H. Powell, Professor Emeritus, University of California at Berkeley, that helped a lot in this project conception.

Tables of contents

List of figures.....	iii
List of tables.....	vii
List of variables.....	ix
Chapter 1 - Introduction.....	1
1.1 - The problem of pallet racking systems.....	1
1.1.1 - Overview	1
1.1.2 - The international situation.....	4
1.1.3 - Overview of damage to steel pallet storage racks and content spillage.....	7
1.2 - State of art of seismic research on storage racks	11
1.2.1 - Experimental researches	11
1.2.2 - Analytical and numerical researches	12
1.2.2.1 - Linear modeling.....	13
1.2.2.2 - Non linear modeling	14
1.2.3 - Research needs.....	14
1.2.3.1 - Experimental research needs	15
1.2.3.2 - Analytical research needs	16
1.2.4 - Scope and aim of the research.....	16
1.3 - The SEISRACKS project.....	16
1.3.1 - Objectives of the project	16
1.3.2 - Component tests.....	19
1.3.2.1 - Beam-to-upright connections	20
1.3.2.2 - Column base connections	21
1.4 - Organization, scopes and aims of this work.....	23
Chapter 2 - Experimental program	25
2.1 - The SEISRACKS experimental specimens.....	25
2.2 - Experimental structural components	26
2.3 - Experimental shaking-table tests	27
2.4 - Test specimens	28

2.4.1 - Specimen A1	28
2.4.2 - Specimen A2.....	29
2.4.3 - Specimen A4.....	30
2.5 - Experimental results	30
2.5.1 - A1 and A2 specimen (down-aisle direction analysis)	30
2.5.2 - A4 specimen (cross-aisle direction analysis).....	33
2.6 - Experimental failure modes	36
2.6.1 - A1 specimen	36
2.6.2 - A2 specimen	38
2.6.3 - A4 specimen	38
2.6.4 - Failure modes conclusions	40
2.7 - Conclusions	40
Chapter 3 - Numerical simulation	41
3.1 - The software	41
3.2 – Preliminary studies	42
3.3 - Numerical “SEISRACKS” model	57
3.3.1 - Model description.....	57
3.3.2 - Numerical shaking table tests	61
Chapter 4 - Accuracy of the numerical model	65
4.1 - A1 specimen.....	65
4.2 - A2 specimen.....	68
4.3 - A4 specimen.....	72
4.4 - Conclusions	76
Chapter 5 - Conclusions	77
5.1 - General conclusions	77
5.2 - Future development.....	78
References	81

List of figures

Figure 1 - Typical pallet rack configuration (SEISRACKS, 2007).	1
Figure 2 - Storage rack example (SEISRACKS, 2007).....	2
Figure 3 - Storage rack example (SEISRACKS, 2007).....	3
Figure 4 - Public warehouse store (FEMA460).	4
Figure 5 - Storage rack example.	5
Figure 6 - Damaged pallet (or non-allowed/non-standard pallet type) (SEISRACKS, 2007).	8
Figure 7 - Damaged uprights due to industrial truck collisions (SEISRACKS, 2007).	8
Figure 8 - Fork-lift truck collision on beams in a low passage way (SEISRACKS, 2007).....	8
Figure 9 - Serious calamity at the passage way. Fortunately, the roof of the truck fulfilled its protective function (SEISRACKS, 2007).	9
Figure 10 - Collapse due to human error, despite the use of (VNA) trucks (SEISRACKS, 2007).9	
Figure 11 - Examples of “Domino – effect” (SEISRACKS, 2007).	9
Figure 12 - Examples of collapse in “drive-in” structures (SEISRACKS, 2007).....	10
Figure 13 - Examples of collapses with goods spilled over the fork lift trucks (SEISRACKS, 2007).	10
Figure 14 - Typical proprietary moment connection.	18
Figure 15 - Typical bracing members and connections.	18
Figure 16 - Typical column base plate connections.	19
Figure 17 - Specimens for beam-to-upright connection tests: a) connection, b) upright (100/20b) (SEISRACKS, 2007).	20
Figure 18 - Asymmetries in the connections: a) beam-to-upright, b) bases (SEISRACKS, 2007).	20
Figure 19 - Details of base plate and base to upright connections (SEISRACKS, 2007).....	22
Figure 20 - The pallets were fixed on supporting beams of specimen A1.	28
Figure 21 - Maximum deformed shapes of specimen A1, during various tests.	31
Figure 22 - Maximum deformed shapes of specimen A2, during various tests.	31
Figure 23 - Typical modal shapes in down-aisle direction a) 1st mode, b) 2nd mode.	32
Figure 24 - Trend of the maximum inter-storey drifts a) at the various levels of specimen A1, during the test sequence b) and of the absolute displacements.....	33
Figure 25 - Trend of the maximum inter-storey drifts a) at the various levels of specimen A2, during the test sequence b) and of the absolute displacements.....	33
Figure 26 - Maximum deformed shapes of specimen A4, during various tests in cross-aisle direction a) central upright b) lateral upright.....	34
Figure 27 - Trend of the maximum inter-storey drifts a) at the various levels of the central upright of specimen A4, during the test sequence b) and of the absolute displacements....	35
Figure 28 - Trend of the maximum inter-storey drifts a) at the various levels of the lateral upright of specimen A4, during the test sequence b) and of the absolute displacements....	35
Figure 29 - Collapse of specimen A1.	36

Figure 30 - Detail of the first level of specimen A1 after collapse.	37
Figure 31 - Collapse of specimen A1: detail of the failure of the upright at the beam-to-column connection at the third level.....	37
Figure 32 - Collapse of specimen A1: detail of the column-base failure.....	37
Figure 33 - Collapse of specimen A4: a) global collapse; b) failure of the bolted connection between diagonal and upright; c) failure of the column-base connections.	39
Figure 34 - Collapse of specimen A4: failure of the beam-to-upright connections in the horizontal plane, and evident pallet sliding.	39
Figure 35 - Initial view of perform 3D (red tools - modeling tools , blue tools - analysis tools) (program display).	42
Figure 36 - One story plane frame structure (program display).	43
Figure 37 - Non linear connector properties (program display).	43
Figure 38 - Push-Over test properties (program display).....	44
Figure 39 - Northridge earthquake accelerogram (program display).	45
Figure 40 - Dynamic earthquake test configuration (program display).	45
Figure 41 - Seismic isolator properties.....	46
Figure 42 - Isolator axes.....	47
Figure 43 - Isolator element.	48
Figure 44 - Isolator model.	49
Figure 45 - Simple one plane frame structure with the seismic device (in blue) (program display).	49
Figure 46 - Seismic device properties definition (program display).	50
Figure 47 - Results of the one story plane frame structure with the seismic device (fixed).....	50
Figure 48 - Results of the one story plane frame structure with the seismic device (sliding).	51
Figure 49 - Three story and two bays plane frame structure – 1.8 meters beam (program display).	52
Figure 50 - Three story and two bays plane frame structure results – 1.8 meters beam.	52
Figure 51 - Three story and two bays plane frame structure – 2.7 meters beam (program display).	53
Figure 52 - Three story and two bays plane frame structure results – 2.7 meters beam.	53
Figure 53 - Comparison between the two different structures.	54
Figure 54 - First simple 3D structure (program display).....	55
Figure 55 - Real model.....	55
Figure 56 - Full rigid link constraint (program display).	56
Figure 57 - Simple 3D model results.	57
Figure 58 - 3D model similar to the SEISRACKS project (program display).	58
Figure 59 - “SEISRACKS” model.	58
Figure 60 - “SEISRACKS” model.	59
Figure 61 - Beam to column connection properties (program display).	59
Figure 62 - Column base properties (program display).....	60

Figure 63 - A1 specimen test accelerogram (test number 13, y direction) (program display). ...	61
Figure 64 - A2 specimen test accelerogram (test number 16 – y direction) (program display). ..	62
Figure 65 - A4 specimen test accelerogram (test number 3 – x direction) (program display). .	62
Figure 66 - A1 comparison between numerical and experimental displacement – third floor.	65
Figure 67 - A1 comparison between numerical and experimental displacement - second floor.	66
Figure 68 - A1 comparison between numerical and experimental displacement - first floor.	66
Figure 69 - Δ III-II Inter-Storey drift numerical/experimental comparison.	67
Figure 70 - Δ II-I Inter-Storey drift numerical/experimental comparison.	67
Figure 71 - A2 comparison between numerical and experimental displacement - third floor.	68
Figure 72 - A2 comparison between numerical and experimental displacements - second floor.	69
Figure 73 - A2 comparison between numerical and experimental displacements - first floor.....	69
Figure 74 - Δ III-II Inter-Storey drift numerical/experimental comparison.	70
Figure 75 - Δ II-I Inter-Storey drift numerical/experimental comparison.	70
Figure 76 - Seismic device mass division (program display).	71
Figure 77 - First mode deformed shape (program display).....	72
Figure 78 - A4 comparison between numerical and experimental displacements - third floor. ..	73
Figure 79 - A4 comparison between numerical and experimental displacements - second floor.	73
Figure 80 - A4 comparison between numerical and experimental displacements - first floor.....	74
Figure 81 - Δ III-II Inter-Storey drift numerical/experimental comparison.	74
Figure 82 - Δ II-I Inter-Storey drift numerical/experimental comparison.	75
Figure 83 - Rack study possibility.....	78
Figure 84 - Other configuration (program display).	79

List of tables

Table 1 - Investigations of storage rack systems and subassemblies. 12

Table 2 - Summary of characteristics of specimens tested on the shaking table 25

Table 3 - Geometrical properties of the members..... 26

Table 4 - Material characteristics. 27

Table 5 - Base column properties. 27

Table 6 - Beam-to-column connection properties. 27

Table 7 - Tests performed on specimen A1. 28

Table 8 - Tests performed in specimen A2. 29

Table 9 - Tests performed on specimen A4. 30

List of variables

A - Area of the element section

d - Beam height

DU - Ultimate displacement

DX - Maximum displacement

EI - Bending Stiffness

F_g - Gravitational load

F_i^- - Negative load corresponding to displacement e_i in cycle i

F_i^+ - Positive load corresponding to displacement e_i in cycle i

f_u - Ultimate stress

FU - Ultimate load

F_y^- - Yield load in the negative range (ECCS)

f_y - Yield stress

F_y^+ - Yield load in the positive range (ECCS)

I_x - Inertia of the section in the “x” direction

I_y - Inertia of the section in the “y” direction

K_0 - Initial stiffness

K_F - Final Stiffness

K_b - Bending stiffness of the beam

L_b - Length of the beam

m - Total number of load steps to be performed with peak deformations equal to or exceeding the yield deformation

M_g - Bending moment due to gravity loads

M_u^- - Ultimate negative moment

M_u - Ultimate moment

M_u^+ - Ultimate positive moment

M_y - Yield bending moment

$S_{j,ini}$ - Initial stiffness

t - Thickness of the element

W_x - Elastic section modulus in the “x” direction

W_y - Elastic section modulus in the “y” direction

ϵ_u - Ultimate deformation

Φ_c - Failure rotation

Φ_u^- - Rotation correspondent to the ultimate negative rotation

Φ_u - Ultimate rotation

Φ_u^+ - Rotation correspondent to the ultimate positive rotation

Φ_y - Yield rotation

Chapter 1 - Introduction

1.1 - The problem of pallet racking systems

1.1.1 - Overview

Despite their lightness, racking carry very high live load (many times larger than the dead load, opposite of what happens for usual civil engineering structures) and can raise a considerable height. For these reasons they have to be properly designed.

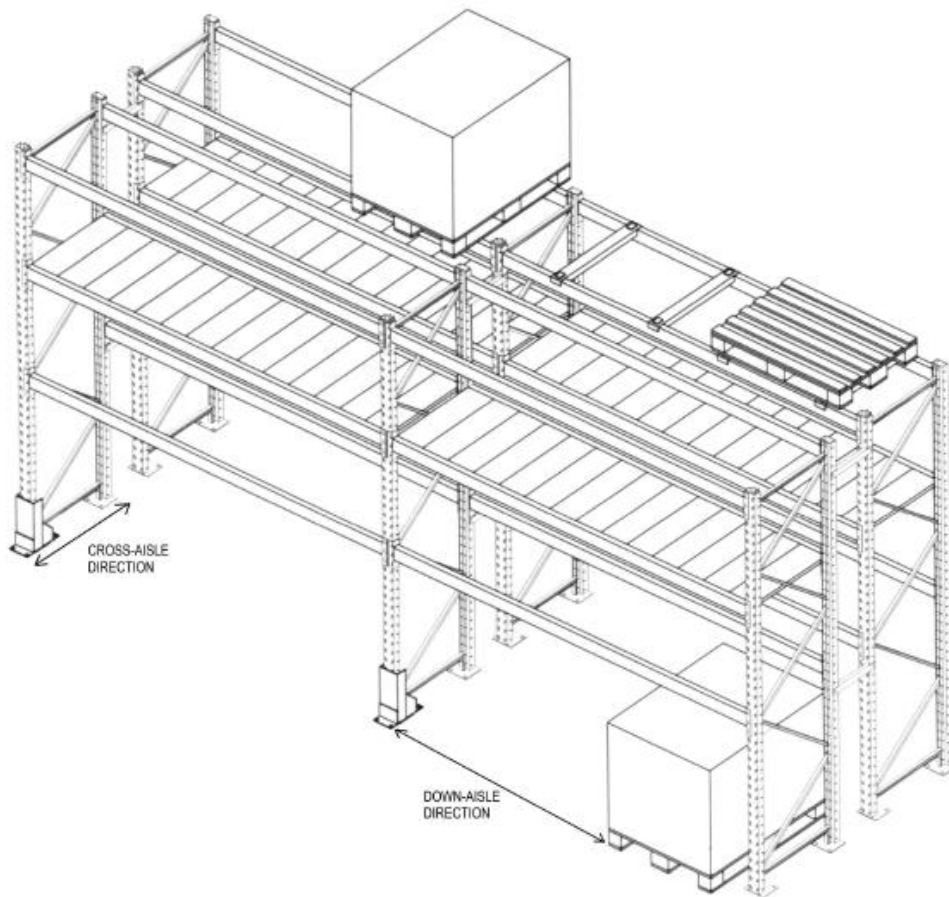


Figure 1 - Typical pallet rack configuration (SEISRACKS, 2007).

Many difficulties arise in the prediction of the structural behavior of pallet racks, like instability (global, local and distortional) or modeling problems (beam-upright connections stiffness, base plate anchoring). The behavior of these systems is affected by the particular geometry of their structural components, made by high slenderness elements, by the non-linear behavior of both the beam-to-column (Agatino, Bernuzzi and Castiglioni, 2001) and by the base-plate joints (Baldassino and Zandonini, 2001).

Therefore, these structures cannot be considered as buildings, and reference cannot be made to usual Structural Design Recommendations and Standards. The most recent Design Standards for steel storage racks (R.M.I. 2002, FEM 2001, RAL 1990, A.S. 1993, FEM 2005) provide a combined numerical/experimental approach in which the design structural analysis is supported by specific tests to evaluate the performance of the key components (members and joints).

The design needs particular attention for storage racks installed in a seismic zone, where they must be able to withstand dynamic forces. Besides the usual global and local collapse mechanisms, an additional limit state for the system is represented by the fall of the pallets with subsequent damage to goods, people and to the structure itself. In Europe, no official document is currently available for the seismic design of pallet racks, and the designers are compelled to operate with a total lack of references and of commonly accepted design rules. Very often they make reference to the Rack Manufacturers Institute (R.M.I.) Specifications (R.M.I., 2002), while the European Federation of Maintenance (F.E.M.) is presently working in order to produce an official document (FEM, 2005).

It must be pointed out that the seismic behavior of steel storage racks is not only a very interesting and challenging problem from a scientific point of view, but it has also a very large economic impact.



Figure 2 - Storage rack example (SEISRACKS, 2007).



Figure 3 - Storage rack example (SEISRACKS, 2007).

Racks, in fact, are widely adopted in warehouses where they are loaded with enormous weight of (more or less) valuable goods. The loss of these goods during an earthquake may represent for the owner a very large economic loss, much larger than the cost of the whole rack on which the goods are stored, or of the cost for its seismic upgrade. Racks are also more and more frequently adopted in supermarkets and shopping centers, in areas open to the public.

The falling of the pallets, in this case, may endanger the life of the clients as well as of the workmen and employees, involving not only Civil and Penal Right considerations about the liability of the owners, but also economic considerations related to the insurance coverage.

In fact, sliding of the pallets on the racks and their consequent fall represents a serviceability limit state i.e. a situation that might occur during a seismic event also in the case of a well designed storage rack, the phenomenon depending only on the dynamic friction coefficient between the pallet and the steel beam of the rack.

Many times, after an earthquake, loss of goods was reported, with or without contemporary failure of the steel rack structural system. Most probably, these structural failures are a consequence of the fall of the pallets and of the impact of the goods on the structure at the lower levels, triggering a progressive dynamic collapse. The uncertainties associated with a clear assessment of the causes of such failures (due to structural design faults or caused by fall of the pallets) may result in long quarrels among constructors, users and insurance companies.



Figure 4 - Public warehouse store (FEMA460).

This brief introduction shows that although these structures, made by thin-walled (and many times cold-formed) steel profiles, are very light and represent only a small percentage of the annual sales of steel profiles in the world, very large economic interests, as well as civil and penal Right liability problems might arise as a consequence of an earthquake event striking them (SEISRACKS, 2007).

1.1.2 - The international situation

During the past few decades, the number of large public warehouse stores (often referred to as big-box stores) has grown significantly, changing both consumer buying habits and the public's risk of injury during earthquakes. Whereas traditional retailers typically store goods and products outside the retail space in limited access storage rooms and warehouse facilities, big-box stores keep goods in close proximity to the consumer at all times. Typically, shoppers in these stores browse in aisles between steel storage racks, 5 to 6 meters in height, that hold pallets of inventory goods, some of which can be very heavy.

During an earthquake, occupant safety in a big-box store depends on both the structural performance of the building and on the performance of the storage racks and their contents. Earthquake ground motions can cause storage racks to collapse or overturn if they are not properly designed, installed, maintained, and loaded. In addition, goods stored on the racks may spill or topple off. Both occurrences pose a life-safety risk to the exposed shopping public.

The seismic design for new warehouse stores, including both the buildings and storage racks, is governed by the building code in force in the jurisdiction where a store is built.



Figure 5 - Storage rack example.

For example, the seismic requirements in building codes currently enforced in most U.S. jurisdictions are based on the *NEHRP Recommended Provisions for Seismic Regulations for New Buildings and Other Structures*, developed by the Building Seismic Safety Council (BSSC) of the National Institute of Building Sciences with National Earthquake Hazards Reduction Program (NEHRP) funding provided by the Federal Emergency Management Agency (FEMA).

The seismic requirements for new stores and storage racks, however, do not stipulate how goods are to be stored on the racks. For example, the state of California has enacted a California Labor Law that requires contents placed on storage racks 4 meters or higher above ground level to be secured. While this law includes a few suggestions for securing goods, it does not include detailed procedures. Thus, in virtually all jurisdictions, requirements for securing storage rack contents are self-imposed by store owners and operators.

The situation is further complicated by the fact that these types of storage racks can be easily reconfigured (i.e., shelf level changed) to meet changing merchandising needs. The reconfiguration work, generally performed many times over the life of the structure, is done by store employees who may not always understand required procedures. Further, fork lifts are used to load goods on the racks and the racks can easily be damaged in the process. Finally,

heavy merchandise stored on the floor near storage racks can topple during an earthquake and damage rack columns and braces, initiating rack collapse.

The stimulus for the development of the *NEHRP Recommended Provisions for Seismic Regulations for New Buildings and Other Structures* was a 2003 request from the State of Washington to FEMA for guidance concerning the life-safety risk posed by the storage racks in publicly accessible areas of retail stores, especially the risk of rack collapse and loss of stored goods during an earthquake. The goal was the possible development of state regulations in response to a fatality resulting from the breaking of a pallet on a storage rack in a commercial retail hardware facility. It should be pointed out that the accident was not associated with an earthquake.

Considering the 2001 Nisqually earthquake, however, the State of Washington recognized that a significant life-safety hazard could be associated with storage racks behavior during earthquakes.

FEMA was aware that current storage rack requirements were somewhat out of date. For example, the latest edition of the storage rack design specification developed in the U.S. by the Rack Manufacturers Institute (RMI) references the obsolete 1994 *NEHRP Recommended Provisions*, even though the *Provisions* document has been updated three times since then (i.e., in 1997, 2000, and 2003). Furthermore, during the 1994 Northridge earthquake (magnitude = 6.7), serious storage rack collapses occurred in several warehouse retail stores that would likely have resulted in injuries and possibly deaths if the earthquake had occurred during a time when the stores had significant public presence rather than at 4:30 a.m. on a federal holiday.

Many existing racks have been since voluntarily strengthened or replaced and stricter quality assurance programs for rack loading and reconfiguration have been implemented by some owners, in order to prevent a reoccurrence of the Northridge problems. In addition, the 1994 *NEHRP Recommended Provisions* included a 50 percent increase of seismic loads for storage racks in areas accessible to the public. FEMA also recognized that the design process must take into account earthquakes larger than those recently experienced.

As already mentioned, in Europe, no official document is currently available for the seismic design of pallet racks and the designers are compelled to operate without references to commonly accepted European design rules. Present Eurocodes 1, 3 and 8 give insufficient information on many design issues.

Recently, rack manufacturers defined a set of conventional design criteria, based on engineering experience, and drafted a “code of good practice” for users, a strict application of which is intended to achieve a safe working environment (FEM 2001). This Code gives insufficient information to some design aspects. Very often designers make reference to the Rack Manufacturers Institute (R.M.I.) Specifications (R.M.I., 2002). In the meanwhile, the

Industry in Europe, under the guidance of the European Federation of Maintenance (F.E.M.) issued a Manufacturers' Design Recommendations called FEM 10.2.02 (FEM, 2001).

These recommended the way in which components are brought together to provide the optimum strength and stability required to store specified pallet load size and maximum weight.

An increasing number of European manufacturers are presently able to design according to these recommendations, if required by their customers. Furthermore, CEN has recently activated a Technical Committee (CEN-TC344), with the aim of developing a set of Eurocodes dedicated to racking and shelving.

1.1.3 - Overview of damage to steel pallet storage racks and content spillage

In 2003, estimated pan-European sale value for the racking industry exceeded 1.2 Billion Euro. Racking systems operated by industrial trucks represent approximately 70% of the total yearly racking industry market. The current estimated yearly loss due to accidental impact is 600 million Euros. Moreover the losses due to consequent fires far exceed this value. Economical losses are expected to continue to rise due to competitive pressure in the logistic industry, resulting in higher driving speeds of industrial trucks within the racking environment.

The warehouse workplace is a potentially dangerous working environment. Careless driving of trucks can cause impact on racking and the dislodgment of loaded pallets onto operatives and even the collapse of part of the racking with its loads. In order to give an idea of the potential economic damage related to a collapse of one of these structures, it is enough to mention as an example that in the last two years, only in the Netherlands, at least two major collapses occurred, with a consequent fire. This fact made things of public domain (which is not usually the case). In these two collapses, there was more than 100 million Euro damage to goods and warehouse.

Fortunately no person killed or injured. In the same period, in Europe, a conservative estimate gives more than 500 million Euro of goods lost due to racking system failures. Moreover, after a failure, the warehouse is usually out of service for a long period, increasing the economic damage.

The following images give a brief overview of possible causes and consequences of storage racks collapses, in daily practice, which include collapse of the pallet that, falling down can cause the collapse of an entire bay of the rack due to the impact, or collision of a fork lift truck with the structure (e.g. Figure 8). Even in case of a more conditioned way of operation (as in case of Very Narrow Aisle (VNA) trucks) human failures can cause a very large accident (Figure 10).



Figure 6 - Damaged pallet (or non-allowed/non-standard pallet type) (SEISRACKS, 2007).



Figure 7 - Damaged uprights due to industrial truck collisions (SEISRACKS, 2007).



Figure 8 - Fork-lift truck collision on beams in a low passage way (SEISRACKS, 2007).



Figure 9 - Serious calamity at the passage way. Fortunately, the roof of the truck fulfilled its protective function (SEISRACKS, 2007).



Figure 10 - Collapse due to human error, despite the use of (VNA) trucks (SEISRACKS, 2007).

In many cases, a partial collapse of part of a rack, results in a global collapse of the racking system in the warehouse, due to a “domino effect”, with a structure falling on the adjacent one (Figure 11).



Figure 11 - Examples of “Domino – effect” (SEISRACKS, 2007).

Of course, failures can occur also in other types of racking systems. Drive-ins are a typology particularly prone to collapses due either to collisions with fork lift trucks, or to global and local stability problems (Figure 12).



Figure 12 - Examples of collapse in “drive-in” structures (SEISRACKS, 2007).

However, one shall never forget that enormous weight of goods are stored above the persons who are daily working between racking, and a failure might cause injuries or losses of human lives.(SEISRACKS, 2007).



Figure 13 - Examples of collapses with goods spilled over the fork lift trucks (SEISRACKS, 2007).

1.2 - State of art of seismic research on storage racks

Experimental and analytical studies of the seismic performance of storage racks are scarce and the results are often proprietary; and consequently, they have not significantly influenced the development of codes and regulations related to storage rack systems.

Available results from experimental and analytical investigations on the seismic response of storage racks are briefly reviewed hereafter, and gaps in knowledge requiring further research studies are identified (SEISRACKS, 2007).

1.2.1 - Experimental researches

Experimental research related to the seismic behavior of storage racks can be categorized into different types of testing procedures:

- *Cantilever* testing of subassemblies in which quasi-static cyclic loads are applied to beam-to-upright connections.
- *Portal* testing of subassemblies in which beam and uprights portal subassemblies are loaded laterally to simulate seismic loading.
- Quasi-static testing of storage rack systems for which completely loaded storage racks are loaded laterally to simulate seismic loading.
- In-situ dynamic testing of storage rack systems with small shakers or under ambient vibrations, in order to obtain their dynamic characteristics (e.g., natural periods and damping).
- Shaking-table testing of storage rack systems, with completely loaded storage racks, excited by recorded or artificially generated ground motions.
- Testing of cold-formed steel members and structures, from which most storage racks are built.
- Testing of merchandise.

Table 1 - Investigations of storage rack systems and subassemblies.

Year	Authors	Testing Types (Number of Specimens)
1973	John A. Blume & Associates	In-situ dynamic test
1979	Krawinkler et al.	Cantilever tests (29), portal tests (6), quasi-static tests of storage rack systems (4), dynamic tests (2)
1980	Chen et al.	Shaking-table tests (4), merchandise tests (2)
2001	Bernuzzi and Castiglioni	Cantilever tests (22)
2001	Filiatrault	Shaking-table tests with real merchandise (5)
2003	Castiglioni et al.	Shaking-table tests (4)
2004	Higgins	Cantilever tests(22)
2004	Filiatrault	Shaking-table tests (4)
2004	Castiglioni	Shaking-table tests with base isolators (2)

Table 1 lists the experimental investigations documented in the public literature, and the various testing techniques.

1.2.2 - Analytical and numerical researches

The seismic response of storage racks in the down-aisle direction is strongly affected by the nonlinear moment-rotation response of the beam-to-upright connections. In the cross-aisle direction, on the other hand, the seismic response of storage racks depends on the characteristics of the bracing members used in the truss configuration. Therefore, numerical models that have been used to predict the seismic response of storage racks incorporate these different lateral load-resisting systems to various degrees. The analytical and numerical research related to the seismic behavior of storage racks can be divided into two different types of models:

- *Linear models* for which the moment-rotation response of beam-to-upright connections is liberalized by simple linear rotational springs representing secant properties at the anticipated response level of the storage racks. For dynamic analysis, an equivalent linear viscous damping model is also used to represent the energy dissipation of these connections during inelastic actions.
- *Nonlinear models* for which the nonlinear response of beam-to-upright connections is followed over the time-history response of storage racks by the use of nonlinear moment-rotation hysteretic rules. This nonlinear modeling is used mainly for research purposes and rarely in design situation.

1.2.2.1 - Linear modeling

John A. Blume & Associates (1973) developed and analyzed equivalent lumped mass numerical models representing selected storage racks in order to compare their predicted fundamental periods to in-situ measured values. Pinned upright bases were assumed for all rack configurations except for the cross-aisle direction of cantilever racks. Rigid beam-to-upright connections were assumed in the down-aisle direction. Reasonable agreement was achieved between measured and computed storage fundamental periods.

Chen et al. (1980) conducted frequency analyses of linear mathematical models in order to compare calculated periods of vibration and mode shapes with those observed during low amplitude shaking table tests and pull-release free-vibration tests that they had previously conducted. These calculated periods and mode shapes were then used to perform response spectrum analyses. The calculated fundamental periods of vibration were also used to determine the base shear coefficients according to the 1973 edition of the Uniform Building Code and to the ATC-3 procedure (ATC 1978). It was found that two-dimensional models with minimum net section properties and centerline dimensions were adequate for practical purposes.

Modeling parameters such as semi-rigid beam-to-upright and base connections should be considered in theoretical predictions of rack response. It was also found that in the down-aisle direction, the lateral forces determined by the 1973 edition of the Uniform Building Code were roughly equivalent to those obtained from response spectrum analyses with intensity levels slightly more than 50% of the 1940 El Centro and 1966 Parkfield earthquake records. In the cross-aisle direction, however, the code lateral forces were approximately equivalent to 25% to 50% of the El Centro and Parkfield records. In the cross-aisle direction the lateral forces predicted by the UBC were higher than those predicted by the ATC-3 (ATC 1978) procedure. Opposite results were obtained in the down-aisle direction.

John A. Blume & Associates (1987) performed static and response spectrum analyses to investigate the applicability of the eccentric braced frame concept (Roeder and Popov 1978) to storage racks in order to improve their seismic behavior in the cross-aisle direction. The results of the study indicated that, aside from a considerable savings in steel material, the eccentric bracing system could undergo significantly more inelastic deformations without structural instability than conventional bracing systems. Although the analytical results were promising, the authors recommended also that experimental investigations needed to be conducted before implementing the eccentric bracing system in storage racks. Such experimental results are not available to date.

1.2.2.2 - Non linear modeling

Chen et al. (1980) developed also two-dimensional non-linear numerical models for standard pallet racks in both down-aisle and cross-aisle directions and compared their predictions to the results obtained from shaking-table tests. In the down-aisle direction, semi-rigid beam-to-upright connections and semi-fixed upright bases were assumed in evaluating their initial stiffness. Bilinear moment-rotation hysteretic rules were considered for the semi-rigid beam-to-upright connections. Second order ($P-\Delta$) effects also were considered in the time-history dynamic analyses. The stiffness of the connections between the beams and the uprights was adjusted in the model to simulate the observed local deformations. The responses predicted by the model were in good agreement with the experimental results. Baldassino and Bernuzzi (2000) conducted a numerical study on the lateral-load response of the steel storage pallet rack systems commonly used in Europe. The results confirmed that the nonlinear rotational behaviour of beam-to-upright connections influenced significantly the response of storage rack systems in the down-aisle direction. Also, the numerical investigation confirmed the significant influence of the base plate connections on the overall rack response in both directions. The authors pointed out the need for test data on the non-linear moment rotation behavior of base upright connections.

1.2.3 - Research needs

As presented in this brief review, the current engineering knowledge base concerning the earthquake safety and vulnerability of storage racks is 20 to 30 years old and is limited to contents and racks unlike many modern applications. The retail industry and the state-of-the art of the design of storage racks have changed considerably in the interim. Large chains of stores now routinely invite the public to shop in a physical environment that formerly was found only in a warehouse, racks have more complex configurations and are taller, and their contents have become heavier. These facts clearly pinpoint to urgent research needs related to the seismic behavior of storage rack systems. In this section, experimental and analytical research that is perceived to be the most urgently needed is briefly listed.

1.2.3.1 - Experimental research needs

Only two full-scale shaking-table testing investigations of storage racks fully loaded have been performed in Europe (Castiglioni et al. 2003) and other three in the United States (Chen et al. 1980, 1980; Filiatrault 2001). There is a need to increase the experimental database of the seismic response of complete storage rack systems through shaking-table testing. The main variables that need to be investigated in such experimental programs are:

- The layout and types of storage racks representing current construction practices and innovative systems such as eccentric bracing.
- The layout and types of merchandise contents.
- The types of seismic restraints (e.g., plastic wraps, screens, ledges, etc.) for contents.
- The structural interaction between neighboring racks.
- The direction of the horizontal seismic input, relative to the rack's orientation (transverse, longitudinal, or non-orthogonal).

As demonstrated by available experimental and analytical results, the seismic response of storage racks in their down-aisle direction is strongly affected by the non-linear response of the beam-to-upright and base plate connections. Since numerous variables enter in the design of these connections, an experimental parametric study on the cyclic response of beam-to-upright and base plate connections is urgently needed.

While the needs of the down-aisle direction are urgent, testing needs in the cross aisle are even more urgent since the understanding of this directions behavior is even less understood. Failures of racks in earthquakes are most commonly reported as cross-aisle failures.

The information on the seismic response of merchandise contents installed in storage racks is very limited. There is an urgent need to conduct shaking-table studies of merchandise. For this purpose, shaking-table testing could be used to simulate the motions experienced by various levels of storage racks during earthquakes. A robust numerical model would be required to develop these input motions. Various merchandise items could be mounted on the shaking-table via a rigid assembly representative of the level on which they are mounted. Various types of merchandise contents would be investigated experimentally under a large number of input motions representative of several seismic hazard levels. Furthermore, these results could be compared with the ones obtained when various types of seismic restraints are introduced. With this information, clear recommendations could be provided on the types of seismic restraint to be used for a particular type of merchandise content.

1.2.3.2 - Analytical research needs.

There is a need to develop a general purpose computer-based numerical model for the prediction of the seismic response of storage racks and contents.

The development of such a general-purpose model requires close coordination and interaction with the experimental work.

1.2.4 - Scope and aim of the research

As clearly understandable from the previous overview, at present, there are technical limitations in the field of safety and design of storage racks in seismic areas: lack of knowledge on actions challenging the structures, lack of knowledge on structural behavior in terms of ductility and of sliding conditions of the pallets on the racks and lack of Standard Design Codes in Europe.

To solve some of these limitations, the EU sponsored through the Research Fund for Coal and Steel an RTD project titled "Storage Racks in Seismic Areas" (acronym SEISRACKS, Contract Number: RFS-PR-03114) (SEISRACKS,2007).

All the objectives and descriptions of this project are described in the next sub-chapter.

1.3 - The SEISRACKS project

1.3.1 - Objectives of the project

The objectives of this project, initiated in December 2004 and terminated in June 2007, were:

- to increase knowledge on actual service conditions of storage racks,
- to increase knowledge on racks' actual structural behavior
- to assess design rules for racks under earthquake conditions.

The research team is composed by the following units: ACAI the Italian Association of Steel Constructors (Coordinator), Instituto Superior Tecnico of Lisbon (P), National Technical University of Athens (GR), Politecnico di Milano (I), University of Liege (B) and the European Laboratory for Structural Assessment (ELSA) of the Joint Research Center of Ispra

(Subcontractor of Politecnico di Milano). The scientific objectives of this project can be summarized as follows:

Increase knowledge on actual service conditions of storage racks collecting data by continuous monitoring of a structure located in a warehouse in seismic area.

These data refer, in particular to:

a) actions (actual live load distribution on the rack, occupancy ratio, vertical loads, accidental actions due to impacts, loading cycles, etc.)

b) structural response (vibrations, frequencies, settlements, permanent deformations, etc.)

Increase knowledge on actual structural behavior of storage racks

a) by definition of the sliding properties of pallets on the racks, as a function of : i) type of pallet, ii) stored material, iii) acceleration, iv) frequency of the excitation

b) by identification of base isolation devices with characteristics suitable to storage racks in seismic areas in order to minimize the pallet sliding phenomenon, and verification by full scale testing of one full-scale base-isolated storage rack

c) by assessment of the actual lateral load carrying capacity and ductility of storage racks by means of pseudo-dynamic tests carried out up to failure of full-scale structures

Assessment of design rules for racks under earthquake conditions

a) by definition of a set of design actions for serviceability and ultimate state design for racks in seismic areas.

b) by definition of q-factors to be adopted in seismic design of racks

c) carrying out a revision of the most updated draft of FEM 10.2.08

Design Standard on the basis of the previous work and collected data, in order to incorporate into the document all the information relevant for a safe, although competitive, design of storage racks in seismic areas.

The research activities to be carried out in co-operation among the partners, in order to achieve the aforementioned objectives within this project, are subdivided in the following Work Packages:

WP 1 – Full scale dynamic tests of storage racks

WP 2 – Full scale pseudo-dynamic and pushover tests of storage racks

WP 3 – In-situ monitoring of storage racks

WP 4 – Cyclic testing of components

WP 5 – Assessment of seismic design rules for storage racks

The project focuses on steel selective pallet storage racks located in retail warehouse stores and other facilities, eventually accessible to the general public.

Storage racks are composed of specially designed steel elements that permit easy installation and reconfiguration consistent with the merchandising needs of a warehouse retail store. Except where adjacent to walls, storage racks normally are configured as two rows of racks that are interconnected. Pallets typically can have plan areas of approximately one square meter and can have a maximum loaded weight of approximately 10-15 KN.

Storage rack bays are typically 1.0-1.1 meter deep and 1.8-2.7 meters wide and can accommodate two or three pallets. The overall height of pallet rack structural frames found in retail warehouse stores varies between 5 and 6 meters. In industrial warehouse facilities, racking system can reach considerable heights, such as 12-15 meters or more.

The rack industry calls the longitudinal direction the down-aisle direction and the transverse direction, the cross-aisle direction. Proprietary moment connections are typically used as the structural system in the down-aisle direction and braced frames are typically used in the structural system in the cross-aisle direction. Photographs of typical down-aisle moment frame connections, cross-aisle braced frame connections, and column base plate connections are presented in Figure 14 through Figure 16.



Figure 14 - Typical proprietary moment connection.



Figure 15 - Typical bracing members and connections.

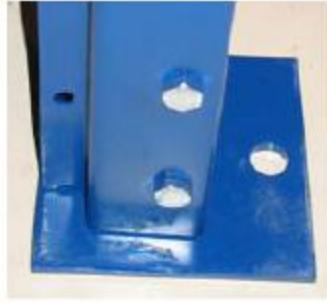


Figure 16 - Typical column base plate connections.

Shaking-table testing of full-scale storage rack systems loaded with real merchandise represents the most direct experimental procedure to assess their seismic behavior. Unfortunately, this type of testing is expensive compared to other methodologies and only a very limited number of shaking-table studies on storage racks have been performed to date in the world and are available in the literature. With the aim of deriving information related to the actual ductility of steel racks and to their ultimate response under strong earthquakes, with the financial support of the EU, Research Programme of the Research Fund for Coal and Steel - Steel RTD, a new Research Project (SEISRACKS, "Storage Racks in Seismic Areas", Contract n. RFS-PR-03114), has been carried out under the co-ordination of the Italian Association of Steel Constructors (ACAI), and the scientific supervision of this author, in cooperation with five European Research Institutions (SEISRACKS, 2007).

1.3.2 - Component tests

Component tests were performed with the aim of characterizing the behavior of both beam-to-upright and base connections, in order to allow a correct interpretation of full scale tests as well as in order to calibrate numerical models. It has to be noticed that the behavior of both components is strongly influenced by the following factors:

- Nature and geometry of the profiles (unsymmetrical cross section of the upright, thin walled sections of both beams and uprights, see Figure 17)
- Asymmetry of the connections. In the case of the beam-to-upright connection, the asymmetry is caused by the inclined hooks and by the presence of the safety-bolt on the upper side of the beam end-plate connector only. In the case of the base connections, the asymmetry is due to the eccentric position of the upright on the base-plate, and by the asymmetrical disposition of the bolts

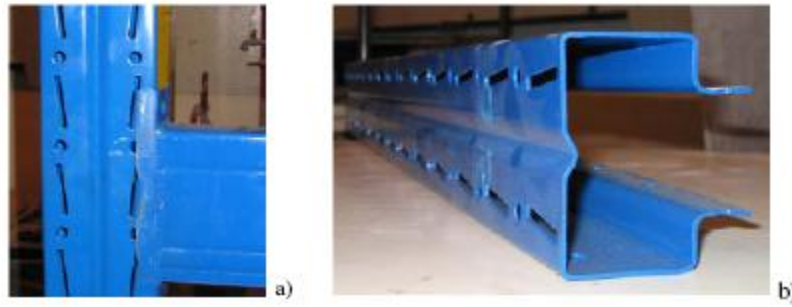


Figure 17 - Specimens for beam-to-upright connection tests: a) connection, b) upright (100/20b) (SEISRACKS, 2007).

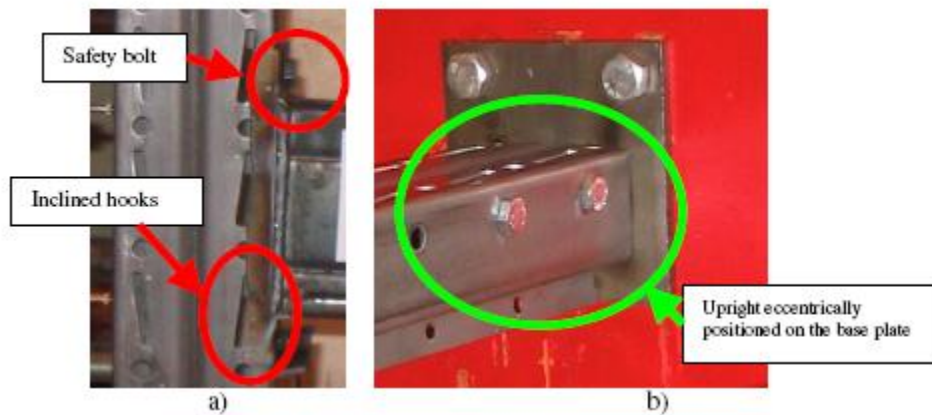


Figure 18 - Asymmetries in the connections: a) beam-to-upright, b) bases (SEISRACKS, 2007).

1.3.2.1 - Beam-to-upright connections

Proprietary moment connections are typically used as beam-to-upright connections for steel selective pallet storage racks. This study focused on the beam-to-upright connection type.

Connection is attained by introducing the hooks in the openings (punched during fabrication) on the uprights, and by adding a safety bolt connecting the upper part of the extended end-plate to the upright.

As a general remark, it should be noticed that this proprietary beam-to-upright connection is strongly non-symmetric in both vertical and horizontal planes.

In the vertical plane, non-symmetry is due to the presence of the safety bolt on the upper side of the beam only and by the fact that the beam is fillet welded to the end-plate on three sides only, leaving the lower flange un-welded.

In the horizontal plane, non-symmetry is due to the shape of the end-plate connector that has hooks on one side only, and is obtained by cold forming of a thin plate, bent in shape of an L, so with a stiffened edge (the same edge where hooks are present).

A non-symmetric response is hence to be expected under hogging and sagging bending.

Objectives of the tests were:

- Assessment of the moment-rotation curves.
- Assessment of the collapse modes of these connections under monotonic and cyclic loads.

1.3.2.2 - Column base connections

Proprietary moment connections are typically used as column-base connections for steel selective pallet storage racks.

The column bases consist of two vertical steel gusset plates fillet-welded to the base plate. The upright is connected to the base by bolting through the slotted holes in the gusset plates using two M10x25 (grade 8.8) bolts for each vertical plate.

The base plate is connected to the foundation surface (in this case either in concrete or in steel) by means of two M16 (grade 8.8) bolts. All bolts are preloaded.

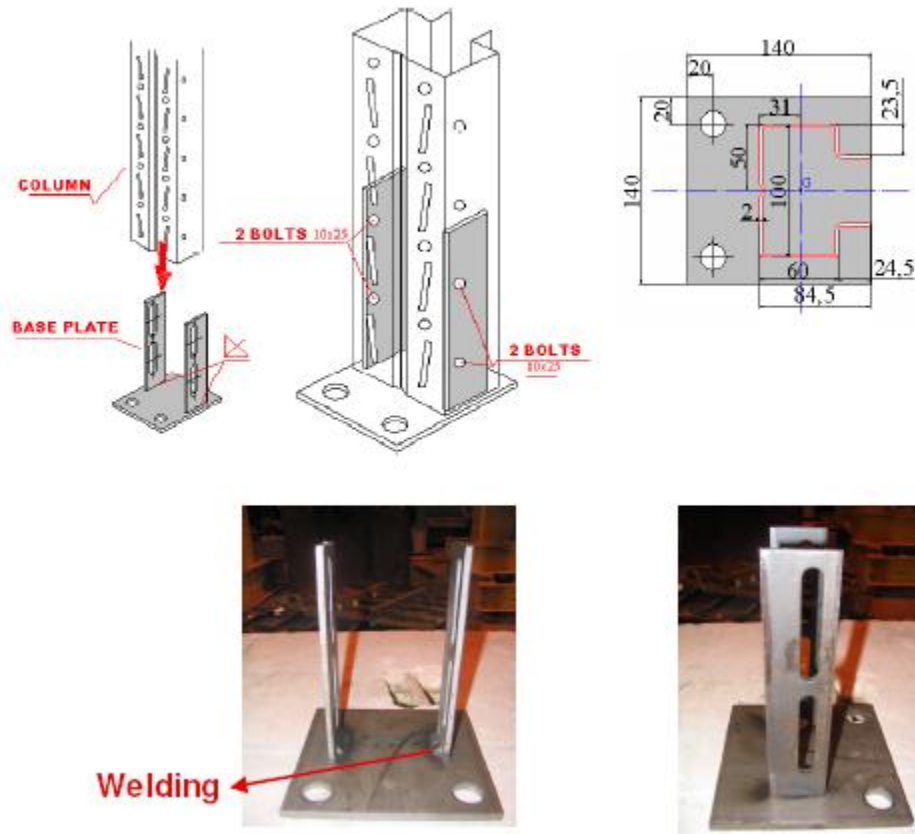


Figure 19 - Details of base plate and base to upright connections (SEISRACKS, 2007).

As a general remark, it should be noticed that this proprietary column-base connection is strongly non-symmetric in cross-aisle direction, where an eccentricity of 66.5 mm exists between the bolt line and the up-right profile.

A non-symmetric response is hence to be expected in cross-aisle direction under transverse load reversals, when the bolts may be either in tension or in compression.

Objectives of the tests on column base connections were:

- Assessment of the moment-rotation curves
- Assessment of the collapse modes

under either monotonic or cyclic transversal loads, for different levels of axial load applied to the upright.

The specimens were tested in the cross-aisle and down-aisle directions. In the cross aisle direction the specimens were subjected to a monotonic load in two different directions, in order to allow respectively tension and compression in the anchor bolts of the column base connection.

1.4 - Organization, scopes and aims of this work

The objective of racking systems behavior and the “sliding of pallets” with a commercial software package “Perform 3D” has been simulated in this work.

The division of the work is made in five chapters:

1. In chapter one it is explained the scopes and aims of this work, the numerical and experimental state – of – art of the pallet racking systems problem and all the “SEISRACKS” project explanation.
2. In chapter two it is explained the entire experimental program, with the description of the loads and the materials – beams, columns, connectors’ characteristics. Some results and conclusions are given to understand the situation of the experimental study.
3. In chapter three is given all the numerical simulation explanation. It is started to be described briefly the features and characteristics of the used program – Perform 3D. Then, it is shown all the preliminary studies and the cases that were used to start working with the program. Some results analysis is done. The last sub-chapter is the “SEISRACKS” numerical model description. All the seismic devices, beams, columns, connectors and the simulation tests are characterized.
4. In chapter four, an accuracy of the numerical model is done, by the comparison between the numerical and experimental results.
5. Chapter five is the conclusion, where general overview of the results of this work is approached.

Generally, it is given an overview of the storage racks situation, including all the needed researches and the scopes of the “SEISRACKS” project. It is explained all the experimental tests, its results and analysis. The next step is focused on the explanation of the numerical model calibration and its specifics. Then, it is tested the accuracy of the model by the comparison between the numerical and the experimental models results. Finally, conclusions and new purposes are given.

Chapter 2 - Experimental program

In this chapter, the experimental program is explained: its specimens, tests and results. According to (SEISRACKS, 2007).

2.1 - The SEISRACKS experimental specimens

Shaking-table tests were carried out on six full-scale rack models, produced by the same manufacturer, affiliated to ACAI, who provided the specimens free-of-charge. All the specimens have two bays, 1.8 m wide, and three levels for a total height of 6.0 m. Neither vertical (down-aisle) nor horizontal (in-plane) bracing systems are present in the specimens that were mainly designed for static loading conditions, without any specific requirement for earthquake loading.

A safety frame was provided capable to sustain both masses and structure in case of collapse or fall of the pallets from the rack. In this way it was possible to perform tests up to collapse, without risk of damaging the testing facility.

The characteristics of each specimen are summarized in Table 2 and will be described in detail in the following paragraphs, as well as the instrumentation that varied from specimen to specimen. At the base, specimens A1, A2, A3 and A4 were bolted and welded on stiff steel plates, which were directly fixed on the shaking table, while specimens A5 and A6 were mounted on proprietary base-isolation systems specifically designed for racking systems in seismic areas (allowing multidirectional in-plane displacements of ± 200 mm), directly provided by two different Italian manufacturers.

Table 2 - Summary of characteristics of specimens tested on the shaking table

Specimen	Beams	N. Levels	Testing Direction	Sliding	Base
A1	130/15	3	Down-Aisle (Y)	No	Fixed
A2	130/15	3	Down-Aisle (Y)	Yes	Fixed
A3	70/15	3	Down-Aisle (Y)	Yes	Fixed
A4	130/15	3	Cross-Aisle (X)	Yes	Fixed
A5	130/15	3	Down-Aisle (Y)	Yes	Isolator_1
A6	130/15	3	Down-Aisle (Y)	Yes	Isolator_2

These were the experimental specimens. In this dissertation, only the problematic specimens are studied - A1, A2 and A4.

2.2 - Experimental structural components

Two different cross-section for beams (S250GD and TG 130x45x1.5) were adopted, with upright of identical cross-section (100/20b). The S250GD was used to the lateral beams and the TG 130x45x1.5 was the configuration of the other beams. The members geometrical properties are shown in the next tables.

Table 3 - Geometrical properties of the members.

Member	Properties	Section
100/20b	A [mm ²]	525.7
	t [mm]	2
	I _x [mm ⁴]	406100
	I _y [mm ⁴]	694680
	W _x [mm ³]	8330
	W _y [mm ³]	14323
TG 130x45x1.5	A [mm ²]	697.66
	t [mm]	1.5
	I _x [mm ⁴]	1742220
	I _y [mm ⁴]	168662
	W _x [mm ³]	26792
	W _y [mm ³]	5171
S250GD	A [mm ²]	141
	t [mm]	1.5
	I _x [mm ⁴]	42873
	I _y [mm ⁴]	9636
	W _x [mm ³]	1965
	W _y [mm ³]	771

The material used for beams and upright is S275 steel, with actual values of yield and ultimate stress showed in Table 2 .

Table 4 - Material characteristics.

Member	f_y [MPa]	f_u [MPa]	ϵ_u (%)
Beam 130x45x1.5	357.0	458.0	27.0
Upright 100x82x2.0	348.0	493.0	25.5

Table 5 - Base column properties.

Base	Axial load [KN]	M_y [KNm]	ϕ_y [mrad]	$S_{j,ini}$ [KNm/rad]
concrete	25.0	2.0	26.3	75.8

Table 6 - Beam-to-column connection properties.

K_y [KNm/rad]	M_y [KNm]	ϕ_y [mrad]	M_u [KNm]	ϕ_u [mrad]
93.65	2.45	25	2.74	120.5

2.3 - Experimental shaking-table tests

A series of uniaxial shaking-table tests along Y or X direction was performed for each specimen.

The time history was an artificial time history which was generated to match the elastic response spectrum Type 1 of EC8 with peak ground acceleration 0.35g, subsoil class D and damping 2%, adequately scaled, from test to test, in order to achieve the desired PGA. In order to adjust to the available displacement capacity of the shaking table, the artificial accelerograms were filtered with a high pass filter 1.0 Hz.

Several shaking-table tests were performed for each specimen with the maximum acceleration of the input signal, along the tested axis, being increased from test to test, until failure of the specimen. A summary of the tests performed for each specimen is given in the next sub-chapter.

2.4 - Test specimens

As it was possible to see before there were tested six specimens. In this thesis will be studied the specimens A1, A2 and A4.

2.4.1 - Specimen A1

Specimen A1 is made with beams type 130x45x1.5 mm and uprights type 100/20b, i.e. of the same types of profiles adopted when characterizing the behavior of beam-to-upright as well as base connections, in the testing campaign carried out at Instituto Superior Técnico in Lisbon.

Table 7 - Tests performed on specimen A1.

Test No	Test Assignment	Direction	PGA [g]	EDA [g]
1	Random Test	Y		
2	Earthquake	Y	0.09	0.084
3	Earthquake	Y	0.21	0.173
4	Earthquake	Y	0.29	0.263
5	Earthquake	Y	0.40	0.355
6	Earthquake	Y	0.50	0.444
7	Earthquake	Y	0.62	0.539
8	Earthquake	Y	0.76	0.633
9	Earthquake	Y	0.87	0.730
10	Earthquake	Y	1.00	0.830
11	Earthquake	Y	1.07	0.931
12	Earthquake	Y	1.18	1.045
13	Earthquake	Y	1.31	1.175
14	Earthquake	Y	1.46	1.313



Figure 20 - The pallets were fixed on supporting beams of specimen A1.

Pallets were rigidly connected to the steel beams, in order to avoid any possible sliding. This was achieved by means of wooden boards, screwed on the beams, on which the wooden pallets were nailed (Figure 20).

Specimen A1 was submitted along the down-aisle direction (the Y main direction of shaking table) to the test history summarized in Table 7, where for each test both the Peak Ground Acceleration (PGA) as well as the Effective Design Acceleration 404 Chapter 6 (EDA) are reported. This parameter corresponds to the peak acceleration value found after low-pass filtering the input time history with a cut-off frequency of 9 Hz (Benjamin, 1988). A total of 14 tests were carried out.

2.4.2 - Specimen A2

Specimen A2 is similar to specimen A1, but the pallets are free to slide on the steel beams, and was submitted along the down-aisle direction to the test history summarized in Table 8.

Table 8 - Tests performed in specimen A2.

Test No	Test Assignment	Direction	PGA [g]	EDA [g]
1	Random test	Y		
2	Earthquake	Y	0.05	0.043
3	Earthquake	Y	0.09	0.082
4	Earthquake	Y	0.15	0.121
5	Earthquake	Y	0.20	0.167
6	Earthquake	Y	0.25	0.207
7	Earthquake	Y	0.30	0.250
8	Earthquake	Y	0.35	0.289
9	Earthquake	Y	0.40	0.330
10	Earthquake	Y	0.43	0.370
11	Earthquake	Y	0.47	0.411
12	Earthquake	Y	0.46	0.411
13	Earthquake	Y	0.54	0.516
14	Earthquake	Y	0.63	0.600
15	Earthquake	Y	0.75	0.668
16	Earthquake	Y	0.86	0.778
17	Earthquake	Y	0.92	0.881
18	Random test	Y		

A total of 18 tests were carried out. After the seismic tests, a random test was executed in order to check any variation of the dynamic characteristics.

2.4.3 - Specimen A4

Specimen A4 is similar to specimen A2 with the pallets free to slide and was submitted, along the cross-aisle direction to the test history summarized in Table 9.

Table 9 - Tests performed on specimen A4.

Test No	Test Assignment	Direction	PGA [g]	EDA [g]
1	Random Test	X		
2	Earthquake	X	0.12	0.089
3	Earthquake	X	0.22	0.176
4	Earthquake	X	0.33	0.264
5	Earthquake	X	0.45	0.350
6	Earthquake	X	0.58	0.440
7	Earthquake	X	0.67	0.533
8	Earthquake	X	0.85	0.627
9	Earthquake	X	0.95	0.717
10	Earthquake	X	1.08	0.806
11	Earthquake	X	1.24	0.894

A total of 11 tests were carried out.

2.5 - Experimental results

In the following, a summary of the main results obtained from the experimental campaign is presented with the aim of allowing understanding of the actual dynamic behavior of steel pallet racks under seismic conditions.

2.5.1 - A1 and A2 specimen (down-aisle direction analysis)

The Figures 21 and 22 show the maximum deformed shapes assumed by the non base-isolated specimens (namely A1 and A2) tested in down-aisle direction during the test series at increasing maximum acceleration of the input motion. Actual values of the Peak Ground Acceleration (PGA), as well as of the Effective Design Acceleration (EDA) corresponding to each test were presented for each specimen respectively in tables 7 and 8.

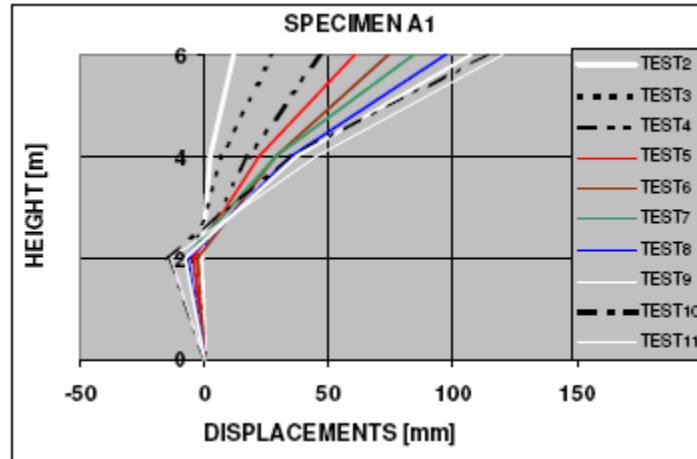


Figure 21 - Maximum deformed shapes of specimen A1, during various tests.

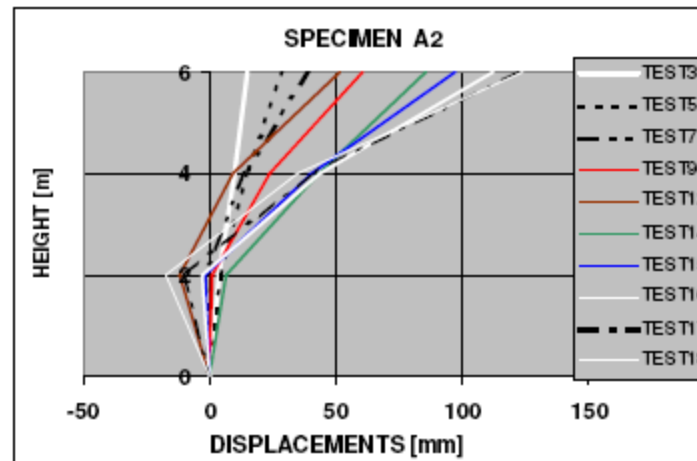


Figure 22 - Maximum deformed shapes of specimen A2, during various tests.

It can be observed that, in down-aisle (longitudinal) direction, the three specimens respond mainly according to the second mode. First mode type of response is evident only for specimen A1 up to test 3 (performed with PGA of 0.21 g) and for specimen A2 up to test 5 (characterized by a PGA of 0.20 g).

Typical modal shapes in down-aisle direction, obtainable by numerical analysis, are shown in Figure 23.

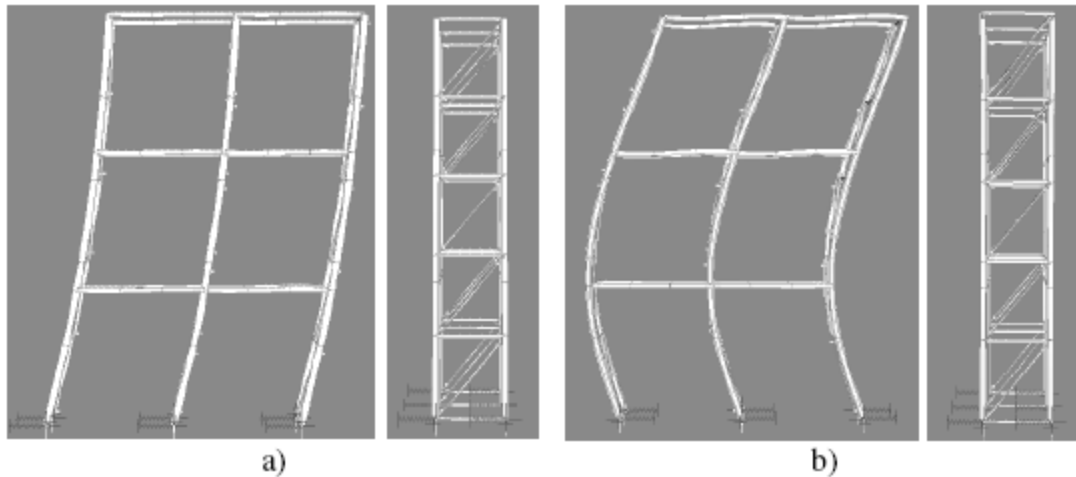


Figure 23 - Typical modal shapes in down-aisle direction a) 1st mode, b) 2nd mode.

The deformed shape of the second mode is such that displacements of the second level are much smaller than those of levels 1 and 3, although the inter-storey drifts are very large, as shown in the Figure 24 and Figure 25. These figures present, for specimens A1 and A2: a) the trend of the maximum values of the inter-storey drift at the three levels (indicated as Δ I-T for the I level, Δ II-I for the second and Δ III-II for the third) as well as b) the trend of the maximum absolute displacements of the same levels together with those of the shaking table, measured during the test sequence.

It is evident that all the two specimens show a similar dynamic behavior. Inter-storey drifts of the first level are always opposite in sign (i.e. in counter-phase) and smaller than those of the upper levels. Test 18 was carried out on specimen A2 with a maximum PGA of 0.92g. Specimen A1 was subjected to a maximum PGA of 1.46g at test 14.

Comparing the maximum displacements of specimen A2 at test 18 with those exhibited by specimen A1 during tests 9 or 10 (carried out at PGA of 0.87g and 1.0g respectively) it can be noticed that deformability of the two specimens is similar.

It can also be observed that the maximum displacements of the first and the third levels are similar to those of the shaking table, while those of the second level are smaller. In the last test, under sustained values of the PGA, a non-linear trend can be observed in the maximum displacements, clearly indicating incipient collapse.

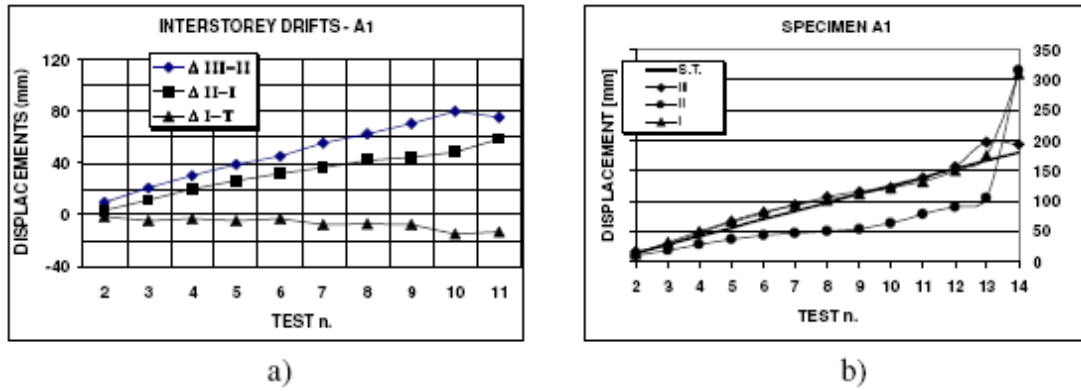


Figure 24 - Trend of the maximum inter-storey drifts a) at the various levels of specimen A1, during the test sequence b) and of the absolute displacements.

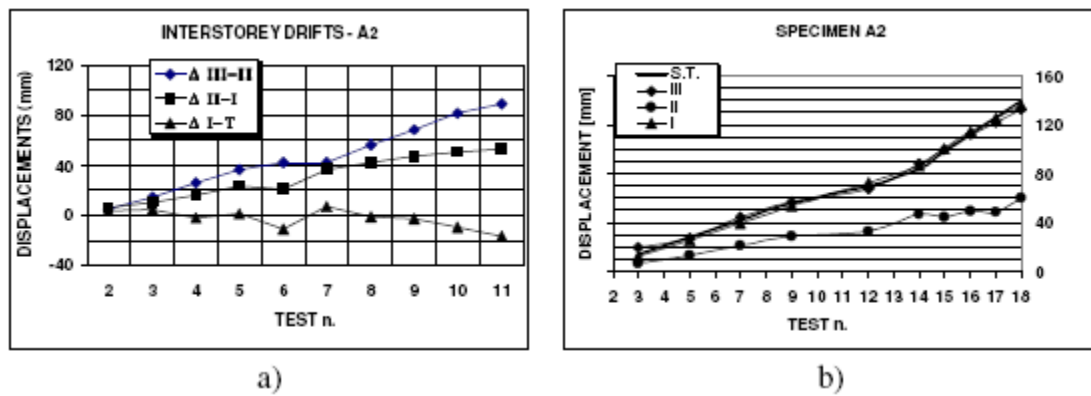


Figure 25 - Trend of the maximum inter-storey drifts a) at the various levels of specimen A2, during the test sequence b) and of the absolute displacements.

2.5.2 - A4 specimen (cross-aisle direction analysis)

Specimen A4, similar to specimen A2, was submitted in cross-aisle direction to the test sequence summarized in Table 9.

Figure 26 shows the maximum deformed shapes assumed by the central (a) and the lateral (b) upright frames during the test series at increasing maximum acceleration of the input motion. The central upright frame, carrying double forces than the lateral ones, shows larger displacements. The deformed shapes of the lateral upright are similar to those of the central frame, but with smaller displacements.

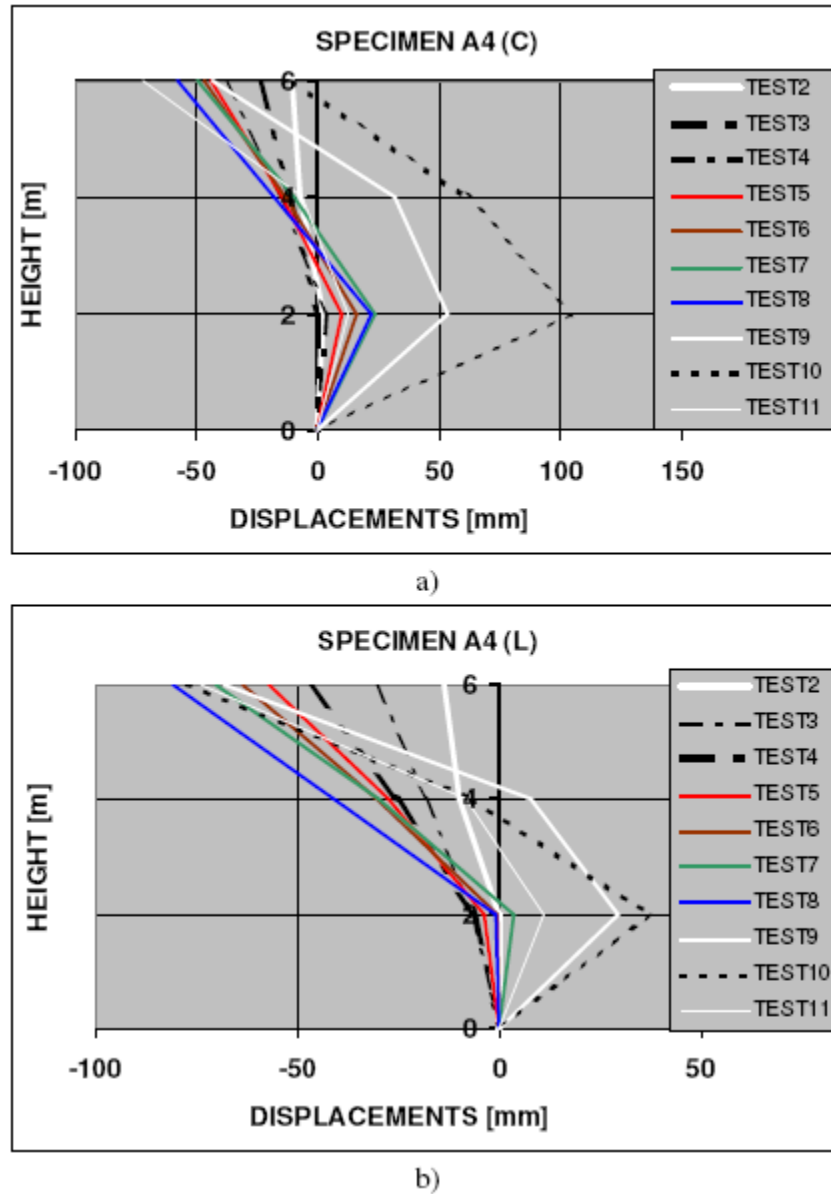


Figure 26 - Maximum deformed shapes of specimen A4, during various tests in cross-aisle direction a) central upright b) lateral upright.

Initially, the structural response is according to the first mode, and the displacements of all three levels are in phase. Increasing the acceleration, during the test sequence, results in plastic deformations at the base of the central upright. Effect of the reduced stiffness of the base connection is a change in the deformed shape, with the displacements of the first and the third level in counter-phase. Rotation of the column base results in an increment of the transversal displacements at the first level. As the deformations of the lateral frames are smaller, the large transversal deformations of the central frame induce, at the beam-ends, very large rotations in the horizontal plane that cause plastic deformations in the beam-to-upright connections. This behavior is also highlighted in Figure 27 and in Figure 28 that show, respectively for the central upright frame and for the lateral one, the trend of the maximum inter-storey drifts (a) and of the

absolute displacements (b) at the various levels of specimen A4, during the test sequence. It can be observed that, up to test 8 (i.e. to a PGA of 0.85g), the inter-storey drift at the first level of the central upright are of the same order of magnitude of those at the above levels. In test 9 (PGA=0.95g , EDA=0.72g) inter-storey drifts show a very large increment. When considering the absolute displacements, Figure 27 highlights that the transversal displacements at level three of the central upright are always larger than those of the shaking table and show a non-linear trend after test 8. The same non-linear increment trend, after test 8, is shown by the displacements at levels one and two that, in the previous tests, were smaller than the shaking-table ones.

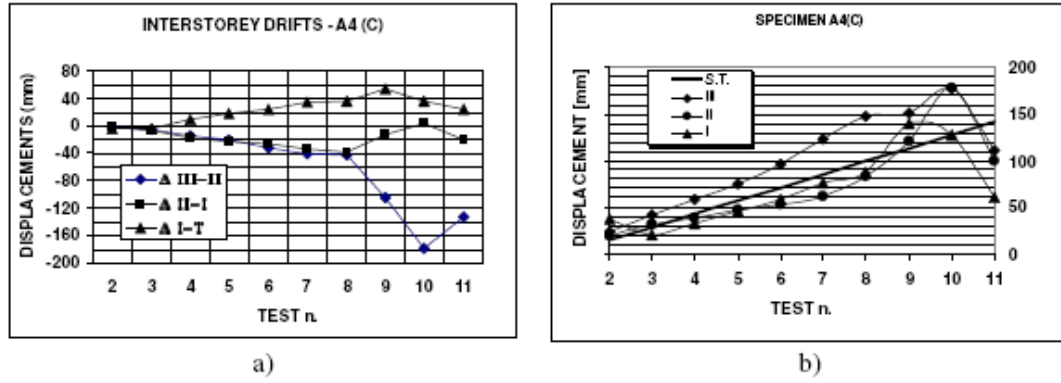


Figure 27 - Trend of the maximum inter-storey drifts a) at the various levels of the central upright of specimen A4, during the test sequence b) and of the absolute displacements.

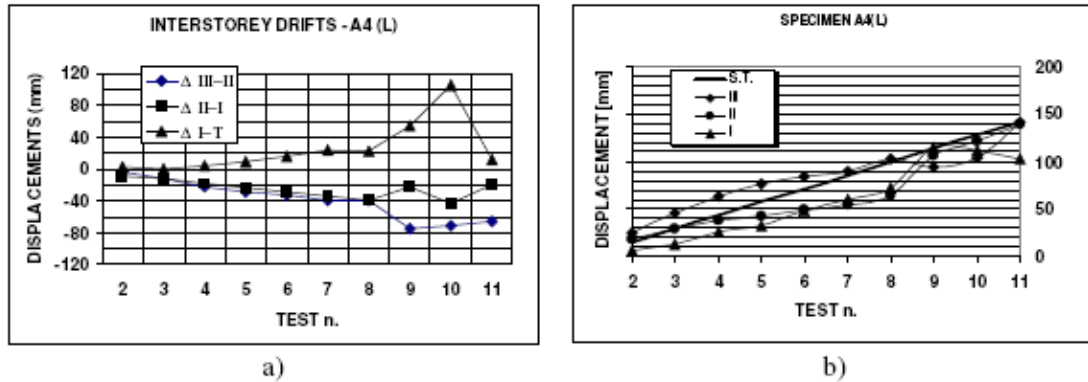


Figure 28 - Trend of the maximum inter-storey drifts a) at the various levels of the lateral upright of specimen A4, during the test sequence b) and of the absolute displacements.

Similar considerations are valid also in the case of the lateral upright frame (Figure 28). In this case, however, during the first 8 tests the inter-storey drifts at the first level are nearly half of those of the upper levels. While the inter-storey drift at the first level is much smaller than that at the same level of the central upright, at the upper levels the inter-storey drifts of lateral and central uprights are comparable.

Comparing the behavior of the lateral and the central upright frames it can be observed that the displacements of the first two levels are similar. At the third level, on the contrary, the displacements of the lateral uprights do not show the large nonlinear increasing trend shown by those of the central one.

2.6 - Experimental failure modes

2.6.1 - A1 specimen

In order to prevent pallet sliding, in specimen A1 wooden boards were connected to the steel beams and the pallets were then fixed on the wooden boards.

The concrete blocks, representing the live loads, were then rigidly fixed to the wooden pallets by means of some steel angles. This choice turned out to be correct in order to eliminate sliding of the pallets, but created some problems, somehow modifying the structural response of specimen A1. Figure 30 shows the deformed shape of specimen A1 after collapse, occurred during test 14. It can be noticed that the structure is hanging on the safety frame.

Evident plastic deformations occurred at the column bases.



Figure 29 - Collapse of specimen A1.

A non-symmetry is however evident in the deformed shapes of the uprights. During the shaking-table tests under high PGA values, in order to accommodate the large inter-storey drift demand,

the upright deformed so much to enter in contact with the concrete blocks, rigidly fixed on the beams.



Figure 30 - Detail of the first level of specimen A1 after collapse.



Figure 31 - Collapse of specimen A1: detail of the failure of the upright at the beam-to-column connection at the third level.



Figure 32 - Collapse of specimen A1: detail of the column-base failure.

Figure 30 shows the plastic deformations occurred in the uprights, at the first level. The central upright highlights a “piece-wise” deformed shape, in its central portion, near the beam-to-upright connection. The presence of the wooden board, rigidly connected to the steel beams increased

the stiffness of the beam. The structure, hence behaved as a strong-beam weak-column system. This resulted in large moments in the upright profiles that suffered plastic deformations. Complete formation of plastic hinges in the columns was avoided on one side because of the reduced stress ratio of the columns (due to presence of two pallets only per bay, instead of the three that are commonly adopted in practical applications for this types of profiles) and on the other side thanks to the semi-rigid behavior of the beam-to-upright connections. In any case, at the third level, shear in the central upright could not be resisted and, near the free, unstiffened, edge the cross-section was severed, fracturing at the openings, as shown in Figure 31. Details of the failure at the column-base connection are presented in Figure 32.

2.6.2 - A2 specimen

The specimen A2 did not present failure modes.

2.6.3 - A4 specimen

Specimen A4 was tested in cross-aisle direction. Neither vertical (down-aisle) nor horizontal (in-plane) bracing systems are present in the specimen that is mainly designed for static loading conditions, without any specific seismic requirement.

As already described, collapse is associated with failure of the central upright frame, that is carrying horizontal forces double than the two lateral uprights. In absence of an in-plane bracing system, in fact, such forces could not be re-distributed among the three upright frames. The failure mechanism is shown in Figure 33. Collapse interested the column-base connections (Figure 33) as well as the beam-to-upright connections that suffered large plastic deformations in the horizontal plane (Figure 33). Failure occurred for accumulation of deformation in the direction in which diagonal members of the upright frames are in compression.



Figure 33 - Collapse of specimen A4: a) global collapse; b) failure of the bolted connection between diagonal and upright; c) failure of the column-base connections.



Figure 34 - Collapse of specimen A4: failure of the beam-to-upright connections in the horizontal plane, and evident pallet sliding.

However, no evident buckling deformation of the diagonal members could be observed. On the contrary, failure occurred at the bolted connections between the diagonals and the uprights, as shown in Figure 33. Significant sliding could be observed during the tests, as highlighted in Figure 34 (shot at the end of test 11), where relative displacements between pallets and beams are evident.

2.6.4 - Failure modes conclusions

Specimen A4 was tested in cross-aisle direction, while all other specimens were tested in down-aisle direction . Specimen A1 was tested, with fixed pallets, in order to avoid sliding, while in all other specimens pallets were free to slide.

The models were subjected to a sequence of shaking-table simulation tests, progressively increasing the PGA. Failure was attained under high values of PGA, despite the fact that the specimens were mainly designed for static loading conditions, without any specific seismic requirement. In any case, all specimens could sustain an shaking-table simulation test with PGA of 0.60g without relevant damage. This stresses the good performance of very flexible structures.

The importance of structural detailing was also highlighted. Most of the observed failures, in fact, were caused by failure of bolted or welded connections. All these details could be easily improved, at low cost, effectively enhancing the structural performance.

2.7 - Conclusions

A1 and A2 specimens were tested in down-aisle direction and A4 in cross-aisle direction.

The importance of small structural detailing was also highlighted. In most cases, in fact, collapse involved failure of bolted or welded connections.

Chapter 3 - Numerical simulation

In this chapter it is given a short description about the used program, it is explained all the preliminary studies and finally, the description of the SEISRACKS numerical model. The information about the program was kindly provided by CSI Computers and Structures.

3.1 - The software

“PERFORM 3D is a highly focused nonlinear software tool for earthquake resistant design. Complex structures, including those with intricate shear wall layouts, can be analyzed nonlinearly using a wide variety of deformation-based and strength-based limit states.

Model data can be imported directly from ETABS and SAP2000. A wide variety of element types are supported, including beams (with panel zones), columns, braces, shear walls (with openings), floor slabs, dampers, and isolators.

Nonlinear analysis can be static and/or dynamic and can be run on the same model. Loads can be applied in any sequence, such as a dynamic earthquake load followed by a static pushover.

PERFORM 3D provides powerful performance based design capabilities, and can calculate demand/capacity (usage) ratios for all components and all limit states. Performance assessment based on ATC-40, FEMA-356 or ATC-440 is fully automated.

PERFORM 3D output includes usage ratio plots, pushover diagrams, energy balance displays, as well as mode shapes, deflected shapes, and time history records of displacements and forces.”

The program includes two phases: Modeling and Analysis.

The Modeling is the building phase of the program. It has various functions to improve a good modeling.

The Analysis phase can be divided into Structural Analysis tasks, Behavior Assessment tasks and Demand-Capacity tasks. The structural analysis tasks are for defining load cases and running structural analyses. The behavior assessment tasks allow you to examine and check the behavior of the analysis model. The demand-capacity tasks allow to calculate demand-capacity ratios, and hence make decisions about the performance of the structure.



Figure 35 - Initial view of perform 3D (red tools - modeling tools , blue tools - analysis tools) (program display).

3.2 – Preliminary studies

Several models were done with the aim of start studying some components behavior and to understand the structure reactions. It is a progressive study, from the 2D simple model to the 3D model. As it is known, the final objective is the storage rack structure described in chapter 2. Many devices are carefully explained in this sub-chapter due to their importance in the final structure.

The first one was a simple structure with two columns (with three meters each) and one beam (with five meters) – one story plane frame. It was used a standard steel section beam IPE 300 and a inelastic FEMA column with a standard cross section HE200A.

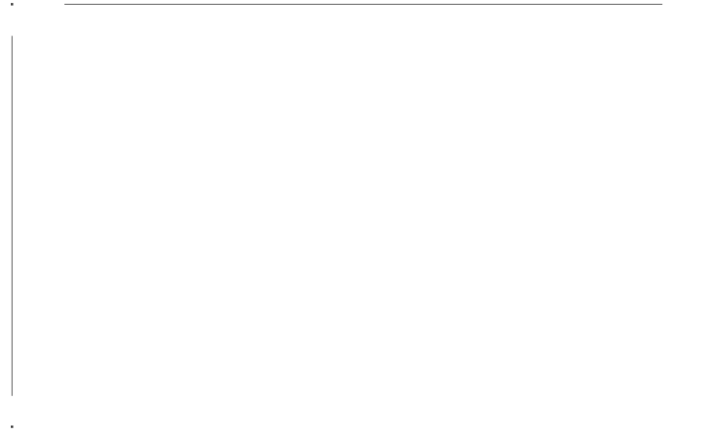


Figure 36 - One story plane frame structure (program display).

There were used moment plastic rotation hinges, adapted to the beam's cross section (IPE 300 as seen in the next figure), considering trilinear effects, symmetry (2D structure), strength loss and without deformation capacities and no cyclic degradation.

In the base (supports) all kind of displacements and rotations were fixed.

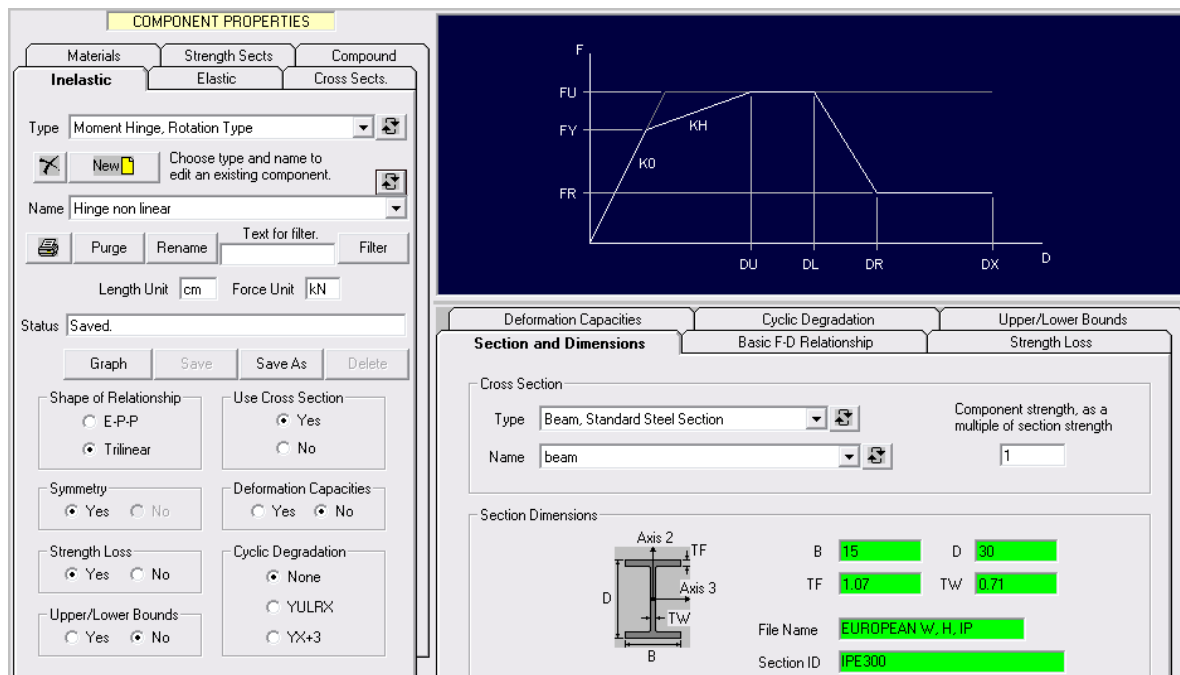


Figure 37 - Non linear connector properties (program display).

This was the first simple structure that was done. The load was defined as 10 KN, in the top of the left column

Then was created the static push-over test with 50 load steps and using the defined load pattern.

LOAD CASES

Load Case Type: **Static Push-Over**

Status: **Saved**

Load Case Name: **Push-Over1**

Analysis Method:
☒ Nonlinear (usual option)
See control information to right.
☐ Linear (currently not allowed)

Load Type:
☒ Nodal Load Patterns
☐ Displacement Pattern
☐ Mode Shapes

Control Information for Nonlinear Analysis

No. of Load Steps: **50**

Max. Events in any Step: **200**

Initial Step to First Event?: ☐ Yes ☒ No

Maximum Allowable Drift (see Controlled Drifts): **0.08**

Limit State to Stop Analysis. Type: **Default**

Name: **Deformation beyond X point for any component**

Reference Drift: **Drift 1**

The reference drift is usually the roof drift relative to the base. It is used as the main deformation measure for plotting push-over analysis results.

Nodal Load Patterns

LOAD PATTERN LIST (MAX. 20) Click to highlight for Insert/Replace/Delete.

No.	Type	Name	Factor
1	Node	load pattern 2	1

LOAD PATTERN TO BE ADDED OR CHANGED

Name: **Load pattern1**

Scale Factor: The sign of the scale factor defines the load direction, and hence the push-over direction.

Add **Insert** **Replace** **Delete**

Figure 38 - Push-Over test properties (program display).

The static pushover analysis is becoming a popular tool for seismic performance evaluation of existing and new structures. The expectation is that the pushover analysis will provide adequate information on seismic demands imposed by the design ground motion on the structural system and its components. It was improved a push-over test to this simple structure to start working with the analysis part of the program.

In this thesis push-over tests aren't developed, they were used to start working with the analysis phase of the program.

To the next structures the used test was a dynamic earthquake defined in the Perform 3D, with the Northridge, 14145 Mulholland, E – W direction. This earthquake has a peak acceleration of 0.5165 g and his accelerogram is in the next image.

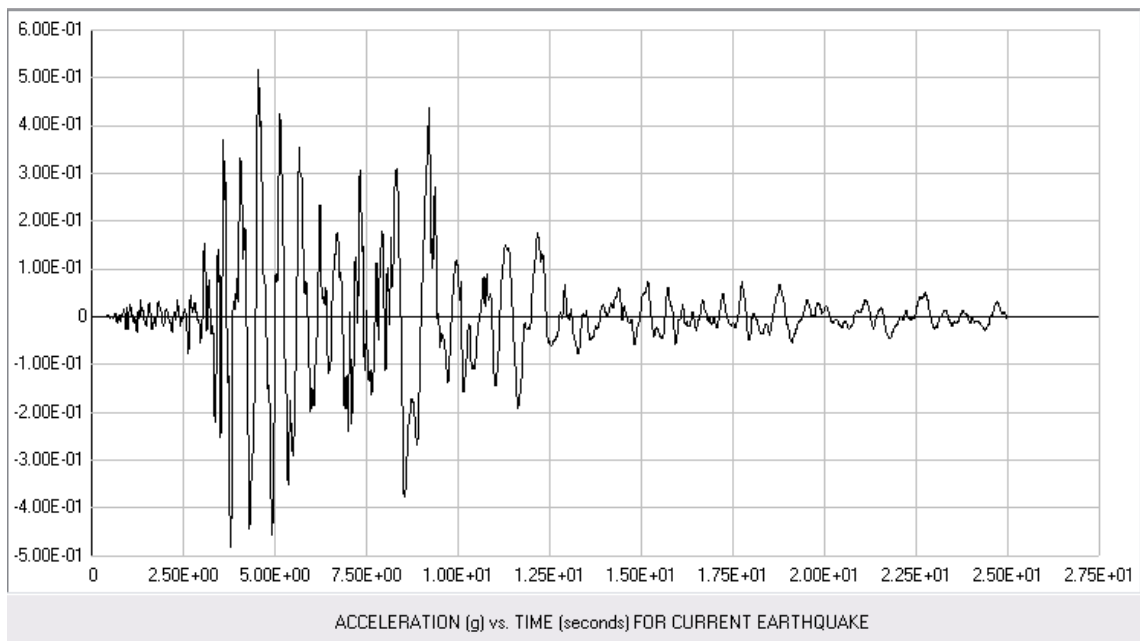


Figure 39 - Northridge earthquake accelerogram (program display).

LOAD CASES

Load Case Type: Dynamic Earthquake

Select name to edit an existing load case.

Load Case Name: EAF2

Status: Saved.

Save Save As Delete UnChange

Add/Review/Delete Earthquakes

Control Information for Dynamic Analysis

Total Time (sec): 15 Time Step (sec): 0.02 Limit State to Stop Analysis. Type: Default

Max Events in any Step (analysis stops if exceeded): 200 Name: Deformation beyond X point for any component

Save results every 1 time steps (default = every step) Reference Drift: Drift 1

This affects time history plots. Usage ratios are still calculated every step. This is used only for "thumbnail" plots of the response.

Earthquake Direction in Plan

Angle from structure H1 axis to earthquake Q1 axis (degrees): 0

Q1 Earthquake

Group: Examples Name: Northridge, 14145 Mulholland, E-W

Peak Acceln (g) = 0.5165 Duration (sec) = 25 Acceln Scale Factor 1 Time Scale Factor 1

Q2 Earthquake

Group: NONE Name:

Peak Acceln (g) = Duration (sec) = Acceln Scale Factor 1.0 Time Scale Factor 1.0

V Earthquake (usually not applied)

Group: NONE Name:

Peak Acceln (g) = Duration (sec) = Acceln Scale Factor 1.0 Time Scale Factor 1.0

Figure 40 - Dynamic earthquake test configuration (program display).

The dynamic earthquake test was used to perform the load case, with the total time of 15 seconds, time step 0.02 seconds and 200 steps maximum.

The next structure was similar to the first one. It was introduced a seismic device to start simulating the pallet behavior, and its contact and friction with the beam. Over this seismic device, a 10 KN load was performed.

The used device is very important to the rest of the models, due to its function of “pallet simulator”.

It is described below.

This device is a rubber type isolator component that has bearing and shear properties as shown in Figure 41.

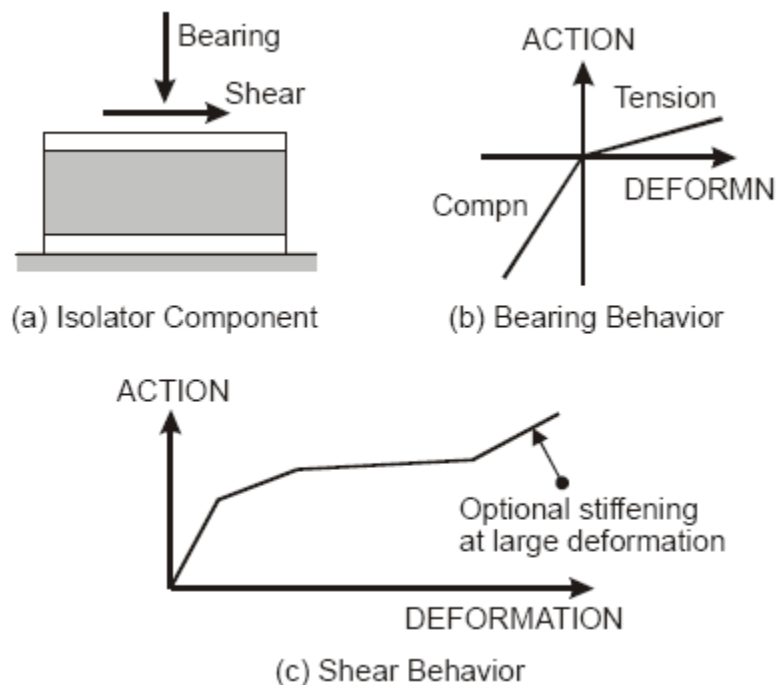


Figure 41 - Seismic isolator properties (CSI Computers and Structures).

The behavior in bearing is elastic, with different stiffness in tension and compression if needed. The behavior in shear is trilinear with optional stiffening at large displacements. There is no strength loss or stiffness degradation in shear. The behavior in shear is independent of the bearing force.

An isolator has three axes, as shown in Figure 42. Shear forces act along Axes 1 and 2. Axis 3 is along the bearing direction. In most cases Axes 1, 2 and 3 will be parallel to the global H1, H2 and V axes, but the axes can be inclined if desired.

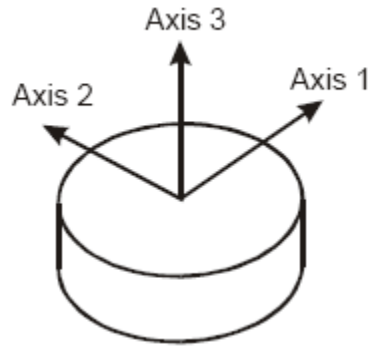


Figure 42 - Isolator axes (CSI Computers and Structures).

If a rubber type isolator component has symmetrical shear properties (i.e., the same properties for shear in any direction) it is assumed to be a typical rubber or lead-rubber isolator with a circular or square shape. For shear forces that are inclined to Axes 1 and 2 the effective shear force and shear deformation are given by:

$$F = \sqrt{F_1^2 + F_2^2} \quad (\text{eq.1})$$

$$D = \sqrt{D_1^2 + D_2^2} \quad (\text{eq.2})$$

where F and D are the effective shear forces and displacements, and F1, F2, D1, D2 are the components along Axes 1 and 2. This is the same as a circular yield surface. The relationship between F and D is as shown in equations 1 and 2.

If a rubber type isolator component has unsymmetrical shear properties (i.e., different properties for shear along Axes 1 and 2) it is assumed to consist of two separate uniaxial devices, one along Axis 1 and one along Axis 2.

Rubber-type isolators are very stiff in compression, but not rigid. It is not good to specify an extremely large bearing stiffness (such as 10^{10}), because it can lead to problems with numerical sensitivity.

Each seismic isolator element connects two nodes (Node I and Node J), and consists of one isolator component plus two rigid links. Figure 43 shows an isolator element.

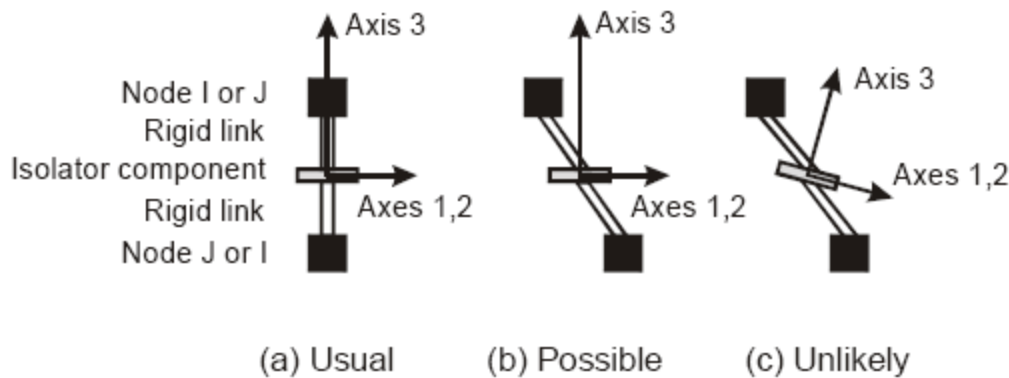


Figure 43 - Isolator element (CSI Computers and Structures).

Nodes I and J will usually be located at the axes of the beams above and below the isolator. The line I-J will usually be vertical, but this is not required.

An important point is that the orientation of Axes 1, 2 and 3 for the isolator component do not depend on the locations of nodes I and J. Instead, it is obligatory to specify the orientations of Axes 1, 2 and 3 directly in the global H1, H2, V coordinate system.

In almost every case, Axis 3 will be vertical (i.e., the shear plane of the isolator will be horizontal) and Axes 1 and 2 will be parallel to the global H1 and H2 axes. In this case will be not need to specify any orientation angles (they are all zero).

The isolator component is placed at a specified point in the element, with the default location at the element midpoint. It is possible to specify the location when is defined the isolator component (not when you define isolator elements).

Since the isolator component has no stiffness in bending, the bending moments at the location of this component are zero. However, the bending moments are not zero at the nodes. For example, for the case in Figure 43 (a), the bending moment about Axis 1 at the node is the shear force along Axis 2 multiplied by the rigid link length. There must be other elements that connect to the nodes and provide bending moment resistance, otherwise the isolator will be ineffective and the structure may be unstable.

Typically the shear force-deformation relationships for rubber type isolators are obtained from tests. The isolator is subjected to bearing force during the test, and hence the measured shear force-deformation relationship includes some geometric nonlinearity effects. The F-D relationship that is specified for the isolator should be based on tests, and hence should account for these effects.

There can, however, be significant $P-\Delta$ moments that are exerted on the members that connect to an isolator. These moments usually need to be considered when designing those members. This section considers these moments and how they can be calculated.

Figure 44 (a) shows, diagrammatically, a rubber type isolator.

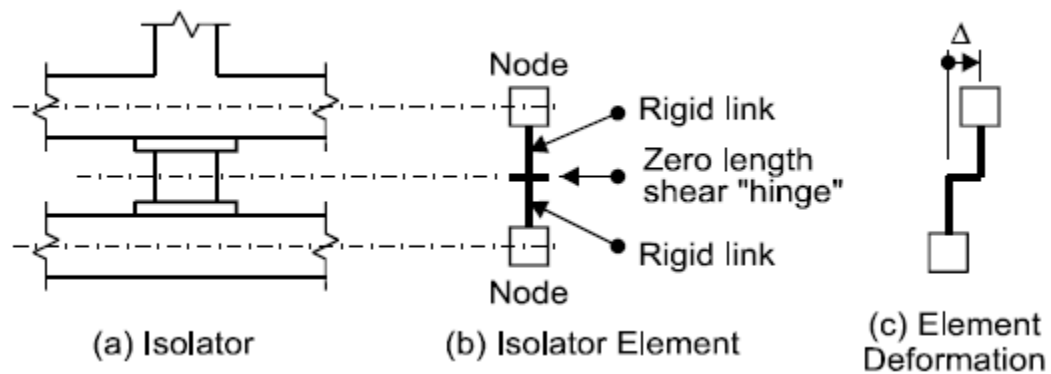


Figure 44 - Isolator model (CSI Computers and Structures).

The analysis model is shown in Figure 44 (b). This element connects to two nodes and consists essentially of an inelastic shear hinge connected to the nodes by rigid links.

The most common mode of deformation for the element is shown in Figure 44 (c). In this case the upper node moves horizontally relative to the lower node (CSI Computers and Structures, 2006).

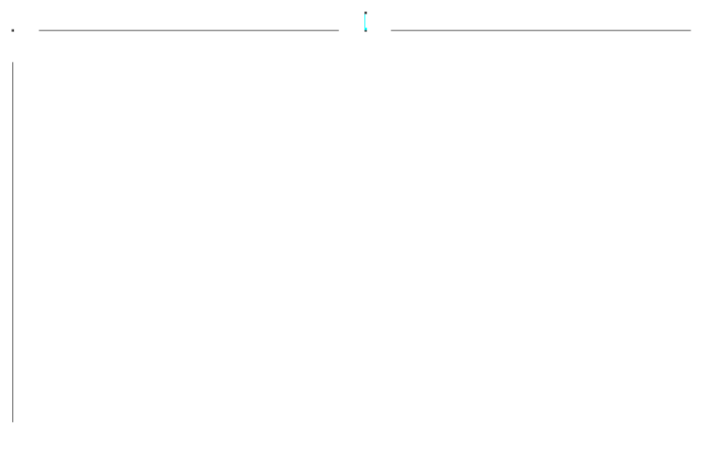


Figure 45 - Simple one plane frame structure with the seismic device (in blue) (program display).

In the figure 46 it is possible to see one example of the definition of the seismic device, by definition of their parameters F_Y , F_U , K_0 , K_F , D_U and D_X .

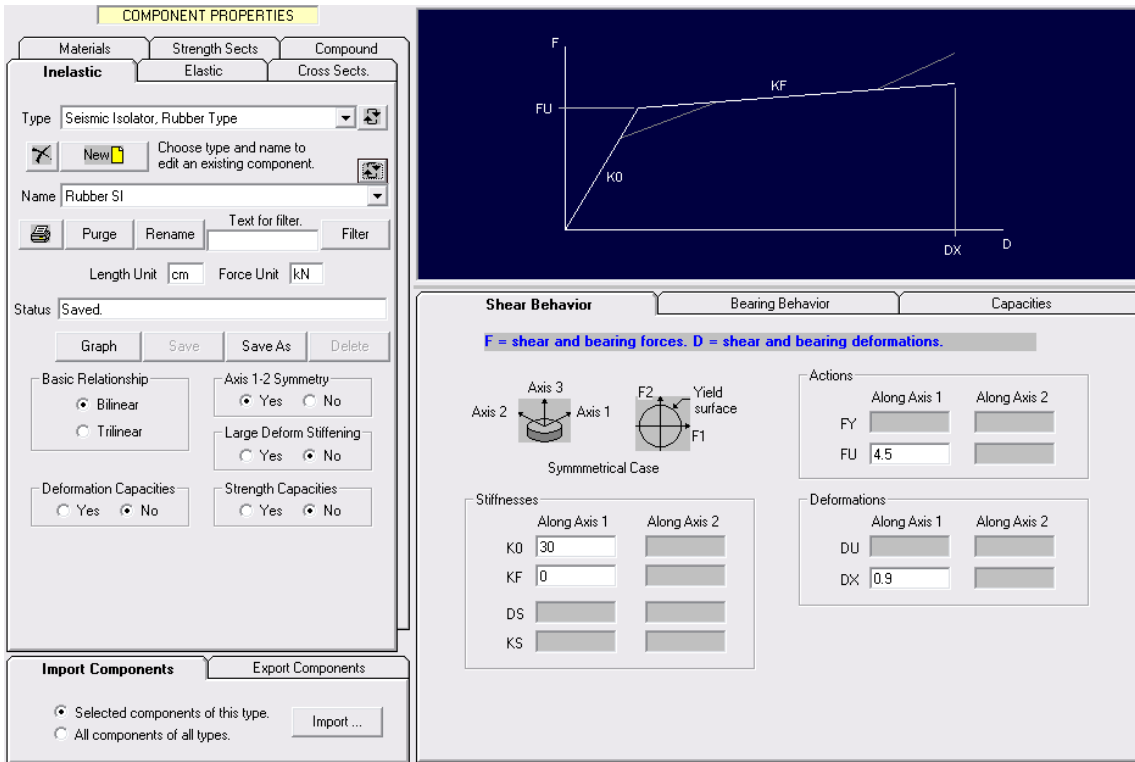


Figure 46 - Seismic device properties definition (program display).

In this first structure (Figure 47) the pallet was initially fixed to the beam.

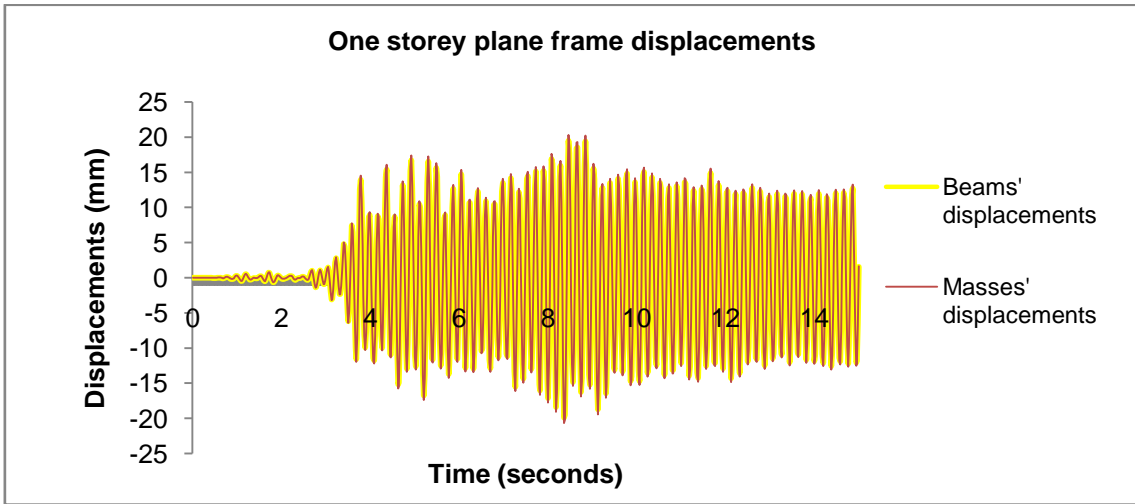


Figure 47 - Results of the one story plane frame structure with the seismic device (fixed).

In yellow there is the beam's displacements and in red the mass's displacements. Naturally, the displacements are very similar because the model is working with the fixed mass and both round the 20 mm maximum.

To begin studying the seismic device's properties it was done the same structure, but the seismic device was configured to slide with a defined acceleration. The used friction coefficient was 0.45 and the results were very interesting.

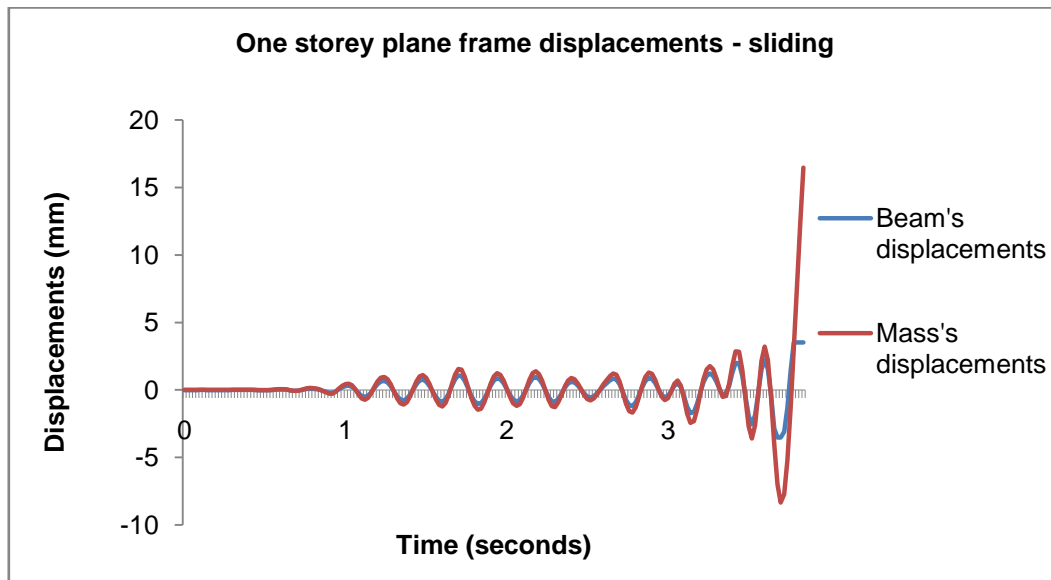


Figure 48 - Results of the one story plane frame structure with the seismic device (sliding).

In blue we have the beam's displacements and in red we have the mass's displacements. As we can see, 4 seconds after the test start (in the higher acceleration part of the test – see Figure 39) the mass slides out of the beam. This shows the good performance of the seismic device configurations.

The next step was doing a three story plane frame structure. The size of the beams was 1.8 meters and 2 meters in the columns. The configuration of the cross sections, the hinges and all structural devices were similar to the SEISRACKS experimental tests – see chapter 2.

In this structure it was configured four masses for each floor, each one of 8 KN (two masses per beam). The seismic device was configured with a friction factor on 0.6 and all the bases were fixed.

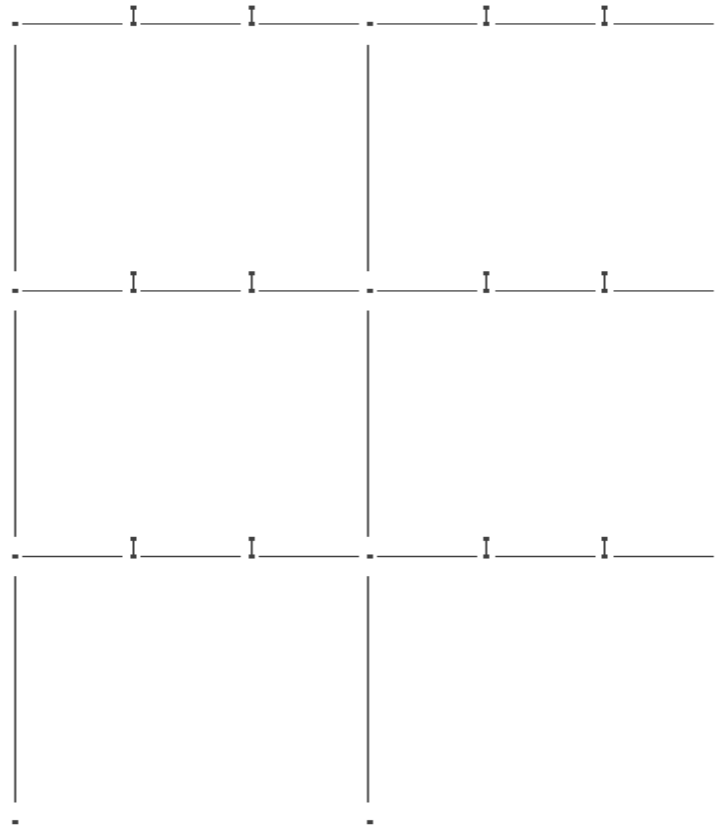


Figure 49 - Three story and two bays plane frame structure – 1.8 meters beam (program display).

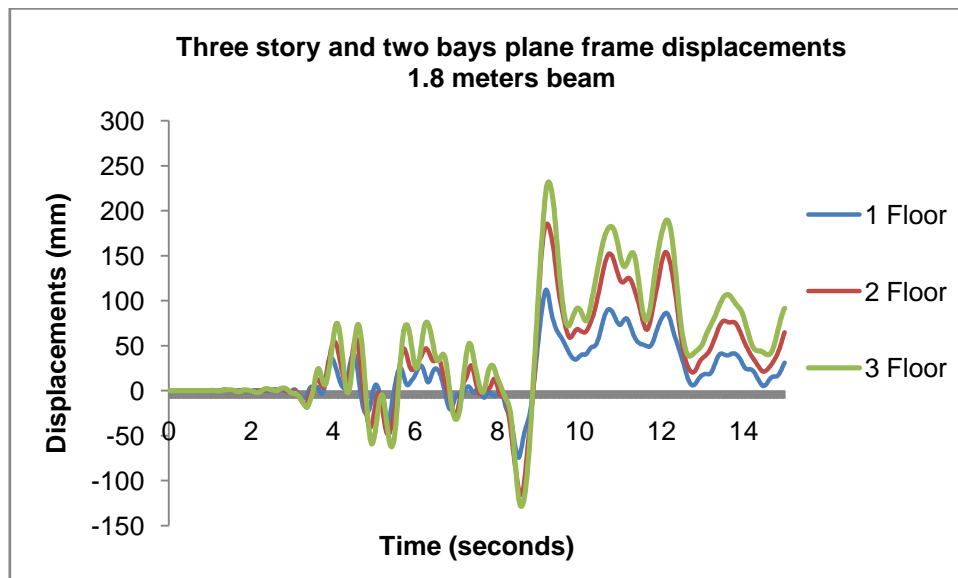


Figure 50 - Three story and two bays plane frame structure results – 1.8 meters beam.

These were the three floors displacements. As it was expected the displacements grow with the floors. The third floor displacement is the bigger one with 200 mm.

The next step was doing a three story and two bays plane frame structure too, but with the variation of the size of the beam – 2.7 meters – and the masses are six per floor - three per beam. This structure was the step before the introduction to the 3D models and it was done to compare the results to the 1.8 meters beam and to study the difference of having a load of 16 or 24 KN for each beam. The used cross section and structural elements were the same.

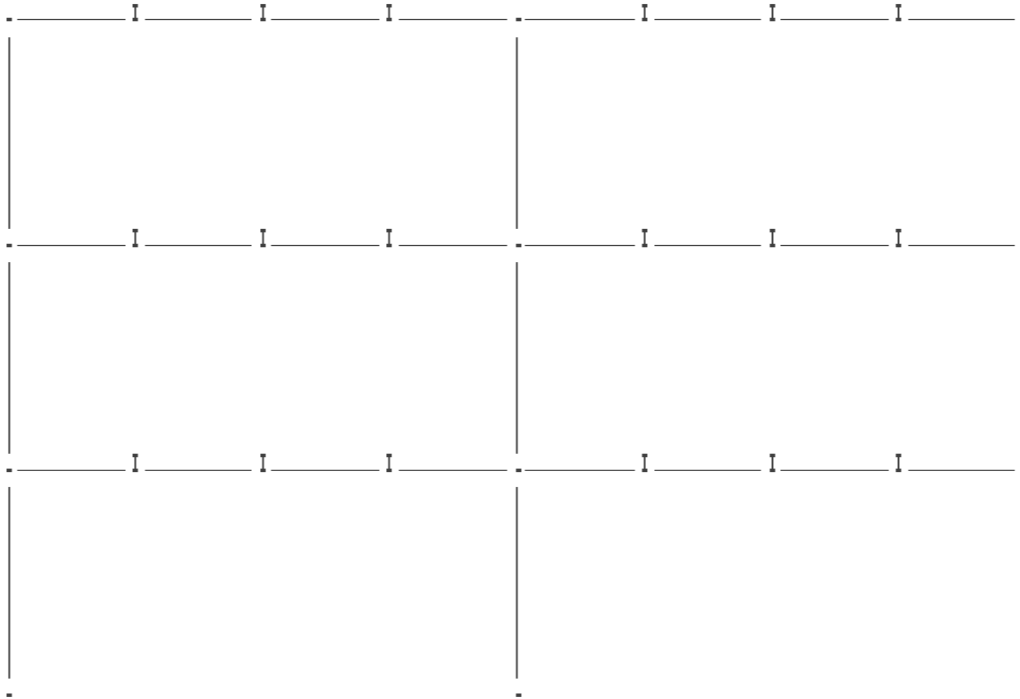


Figure 51 - Three story and two bays plane frame structure – 2.7 meters beam (program display).

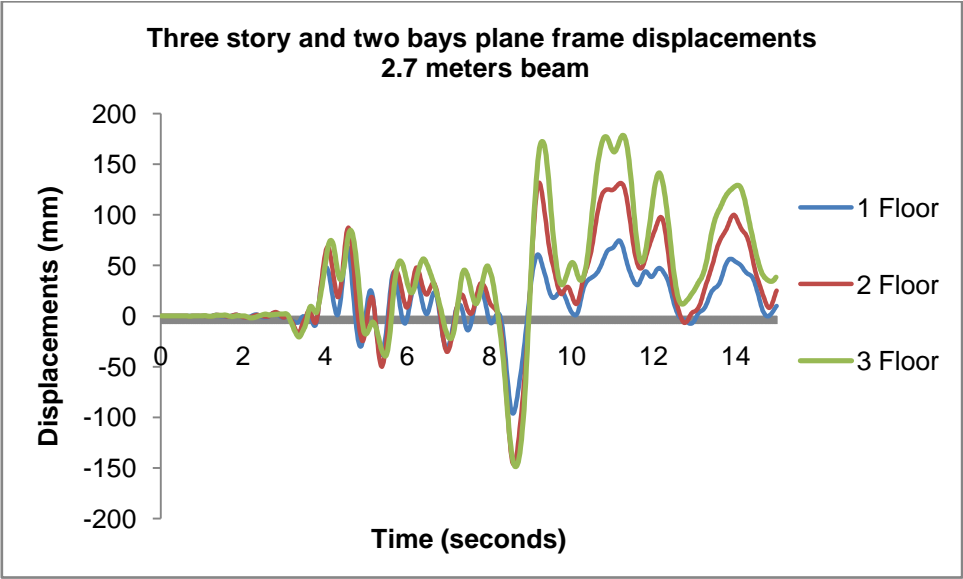


Figure 52 - Three story and two bays plane frame structure results – 2.7 meters beam.

The results were the expected, having different and increasing displacements in the three floors.

It is now interesting seeing the comparison between the two different structures to analyze the beams size and masses influence in the structure response.

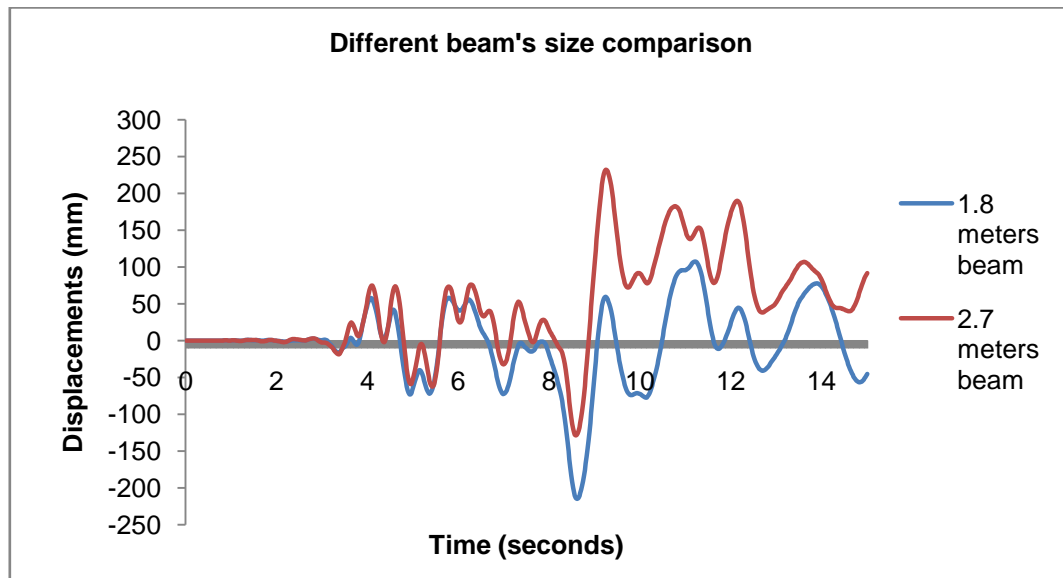


Figure 53 - Comparison between the two different structures.

Naturally, the 2.7 meters beam structure has larger displacements in the 15 seconds of the test. The explanation is in the structures rigidity difference and obviously in masses too. The longest beam structure, correspond to the more flexible the structure.

The last experimental structure that was done, was similar to the structure that was used to do the pallet sliding test (Figures 54 and 55). This was the first 3D structure, and many things had to be redefined in comparison to the 2D models.

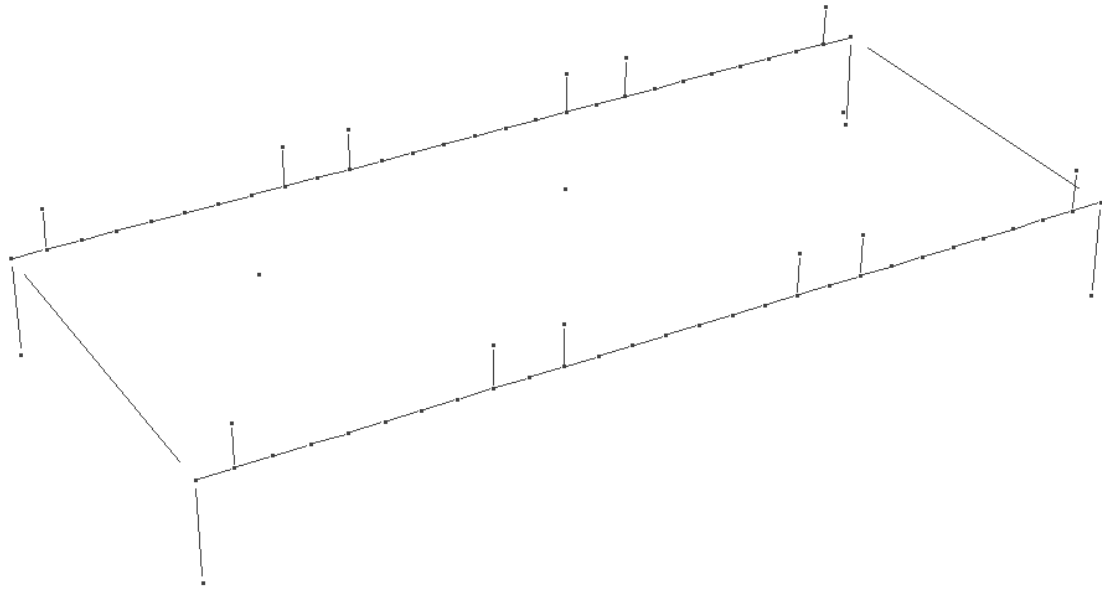


Figure 54 - First simple 3D structure (program display).

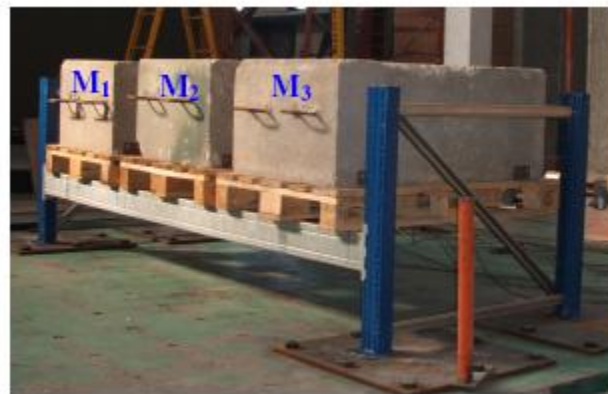


Figure 55 - Real model

This structure has a 2.7 meters beam and 1.2 meters in the cross aisle direction. It was used three loads of 8 kN as it is possible to see in the picture (three central points). To improve the results, it was used a slaving mode to connect rigidly the lateral points (over the beam) to the central point (the mass one). With this slaving mode it was possible to have correct values of the displacements of the masses.

A little explanation of the full rigid link slaving mode is given below.

In a rigid link constraint set, a rigid link is added that connects all of the nodes in the set. The H1, H2 and V translations and rotations are all affected. Specifying a rigid link constraint for the nodes at a floor level, the floor will be rigid both axially and in bending.

Is not possible to include a node in a rigid link constraint if the node has a support of any kind. Correspondingly, is not possible adding a support to a node that is part of a rigid link constraint.

It is very important to be careful with links that are not horizontal. In effect, the constraint links are rigid elements, and they will generally have axial forces, bending moments and shear forces. These forces are not calculated. If a rigid link is vertical or has a vertical component, and if it has an axial force, it may exert a significant P- Δ effect (CSI Computers and Structures, 2006).

There were done three blocks of this kind.

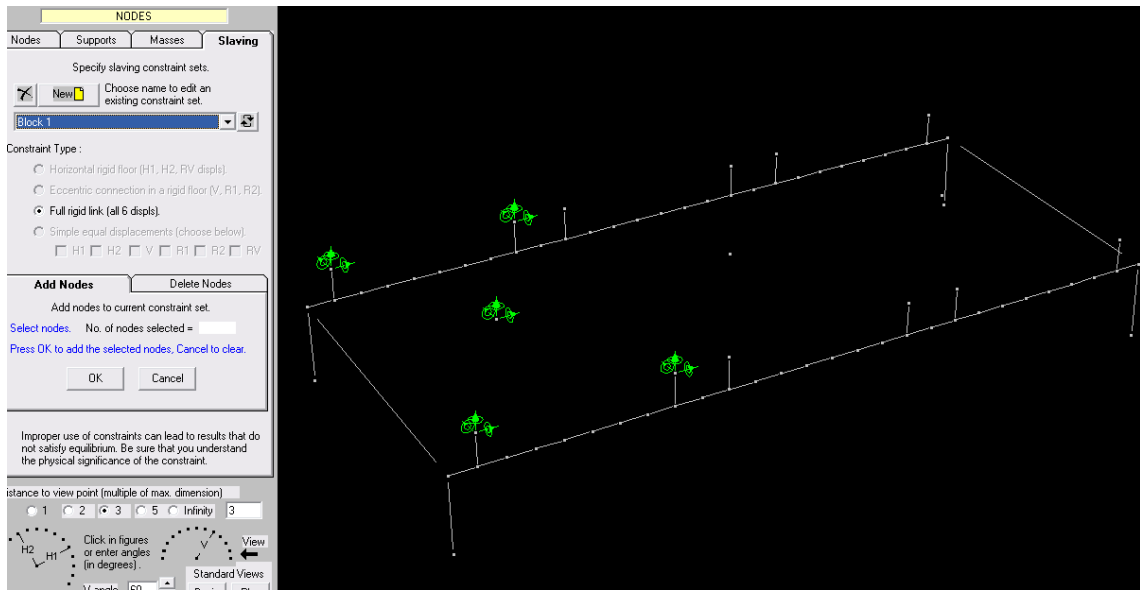


Figure 56 - Full rigid link constraint (program display).

It was improved the same seismic test at this structure and it is possible to see the mass sliding as it was expected.

This model has the function of testing the functionality of the seismic isolator device in the 3D models.

The used friction factor was 0.3 and it is expected the mass to slide out of the pallet – see Figure 57.

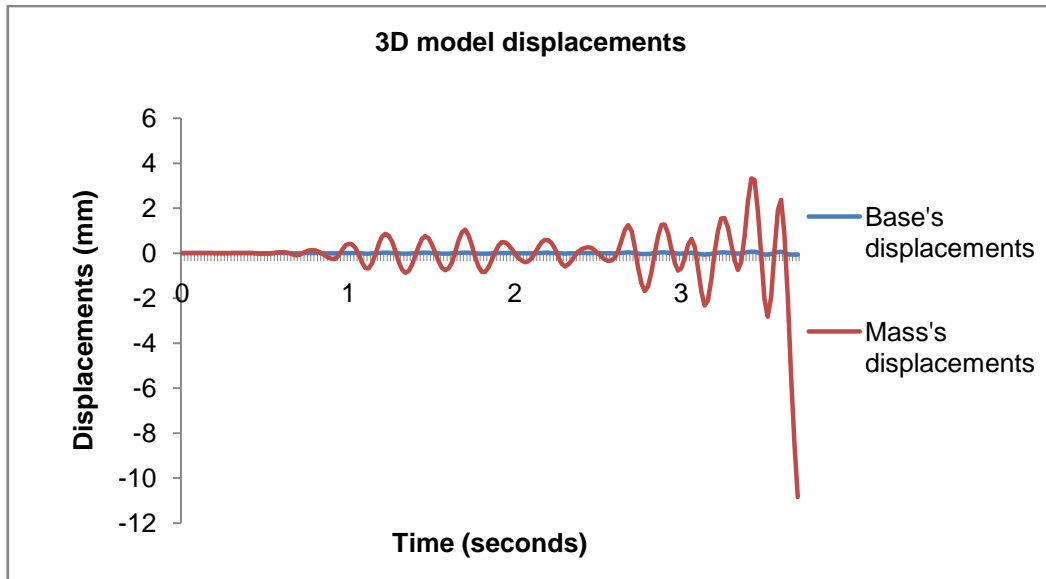


Figure 57 - Simple 3D model results.

The blue line is the base displacements and the red one is the mass displacements. As it was expected, the mass is sliding out of the pallet – that is the reason to the mass's results.

With this test structures or preliminary studies it was done the necessary experiments to start working with the real structures experimented in Athens, Milan, Liege and Lisbon.

3.3 - Numerical “SEISRACKS” model

3.3.1 - Model description

It was performed the three specimens – A1, A2 and A4 - in the PERFORM 3D. The base of the structure is very similar between them. The structure is in the Figure 58.

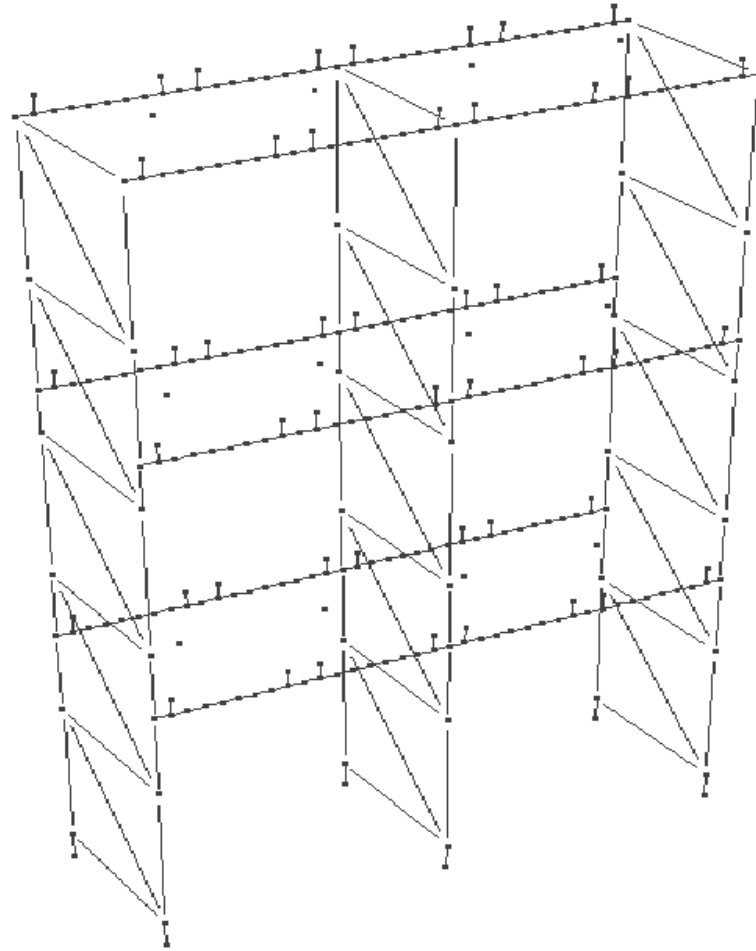


Figure 58 - 3D model similar to the SEISRACKS project (program display).



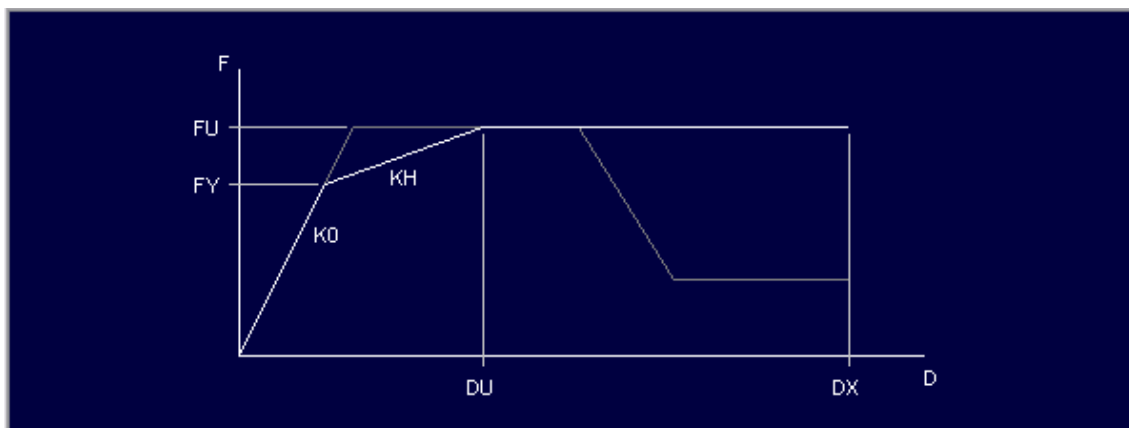
Figure 59 - "SEISRACKS" model.



Figure 60 - "SEISRACKS" model.

The used beams were the TG130x45x1.5 and S250GD and the column was the 100x20b – all those characteristics described in Chapter 2.2.

These were the column and beams definition. All their properties were based in the experimental models beams and columns, as it is possible to see on Table 3 and Table 4.



Positive Actions		Negative Actions	
FY	2.45	FY	
FU	2.74	FU	
Positive Deformations		Negative Deformations	
DU	25	DU	
DX	120.5	DX	

Figure 61 - Beam to column connection properties (program display).

The beam to column connections were defined with the experimental model properties characteristics on the Table 6. The trilinear shape relationship is used and it is defined as symmetric to both sides. It is very important to say that this beam to column connection is used to the A1 and A2 models due to the unawareness of the cross aisle direction properties of the beam to column connection i.e., as it was seen in the next sub-chapter that the A1 and A2 models are tested in the down-aisle direction – all the devices properties are known- and in the case of the A4 model it doesn't occur.

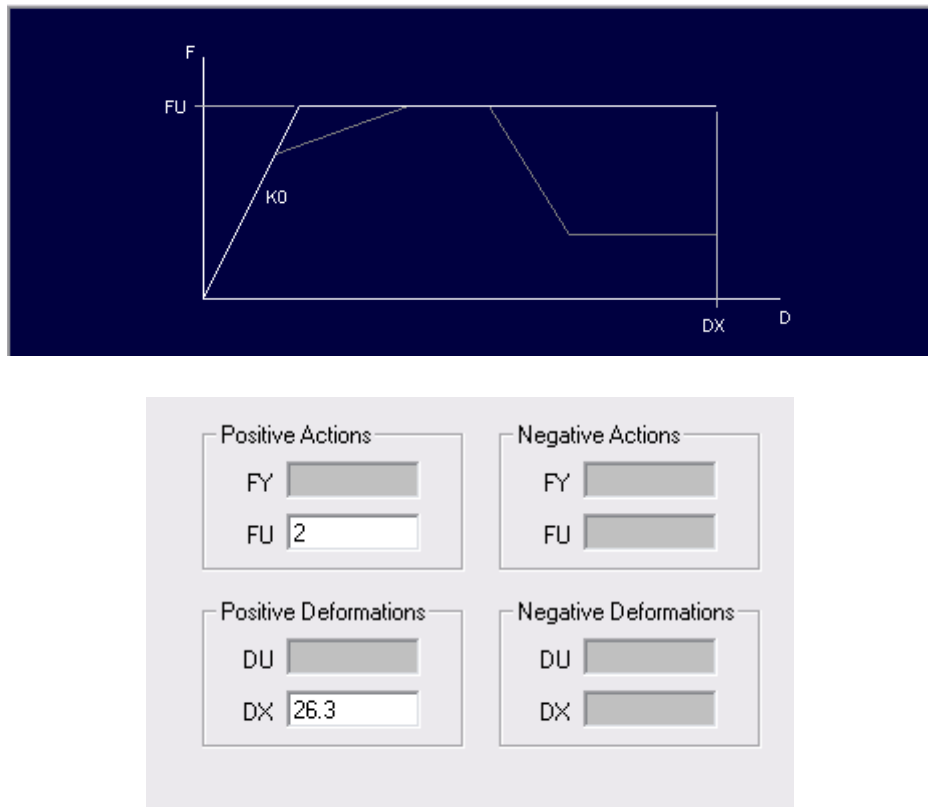


Figure 62 - Column base properties (program display).

The column base properties were the same to the three models and they are shown in the Figure 62. The characteristics are on table 5.

These were the components used to the experimental tests. Their properties were used to define the model in PERFORM 3D. Defining the properties and the materials it is possible to improve and get better results.

3.3.2 - Numerical shaking table tests

In the experimental studies, several tests were done to the specimens, as it was seen before. In this dissertation, it was chosen one PGA for each model and it was improved the test to it.

The tests were done based in the accelerograms of the experimental tests.

In the next figures are the accelerograms used to each test.

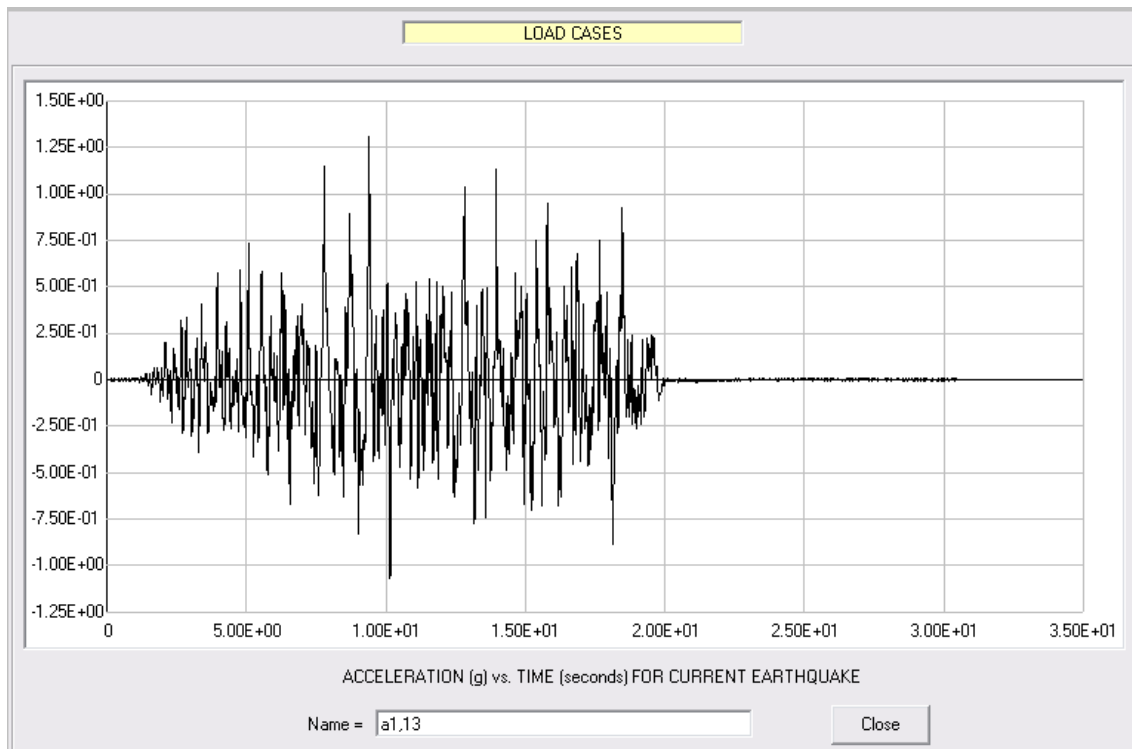


Figure 63 - A1 specimen test accelerogram (test number 13, y direction) (program display).

It was chosen to the A1 model, the 1.31 g maximum acceleration shaking-table test that corresponds to the experimental test number 13 shown in Table 7.

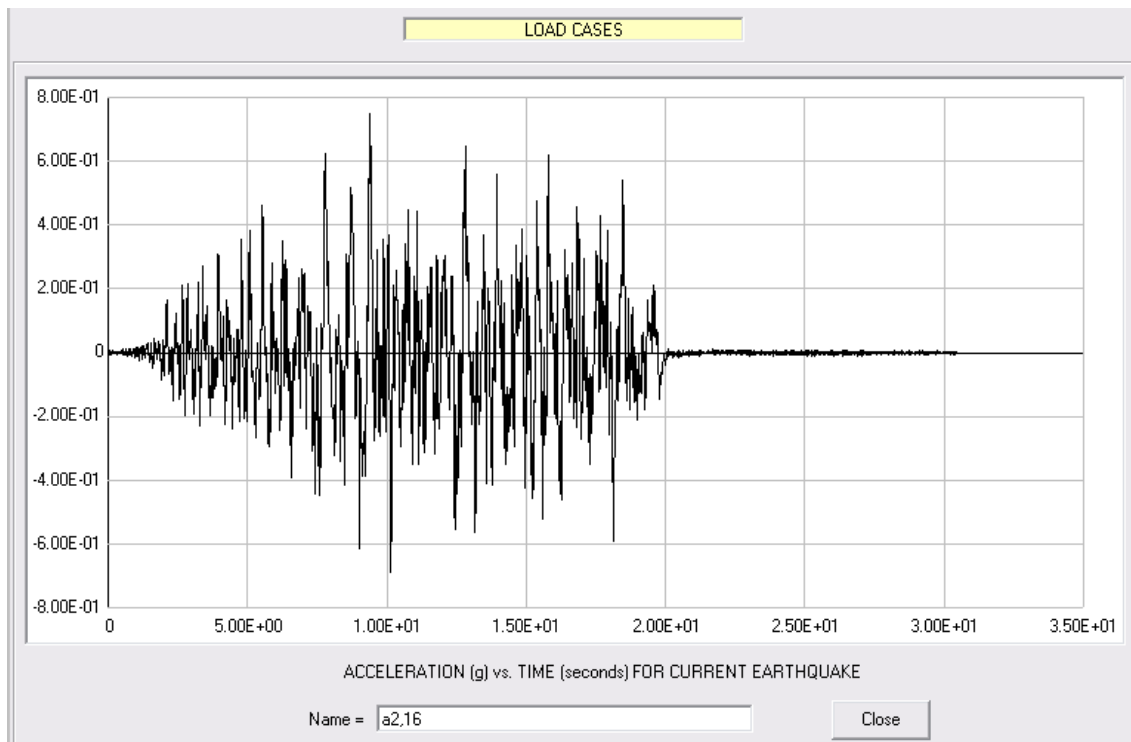


Figure 64 - A2 specimen test accelerogram (test number 16 – y direction) (program display).

It was chosen to the A2 model, the 0.75 g maximum acceleration shaking-table test, that corresponds to the experimental test number 16, as it is possible to seen in Table 8.

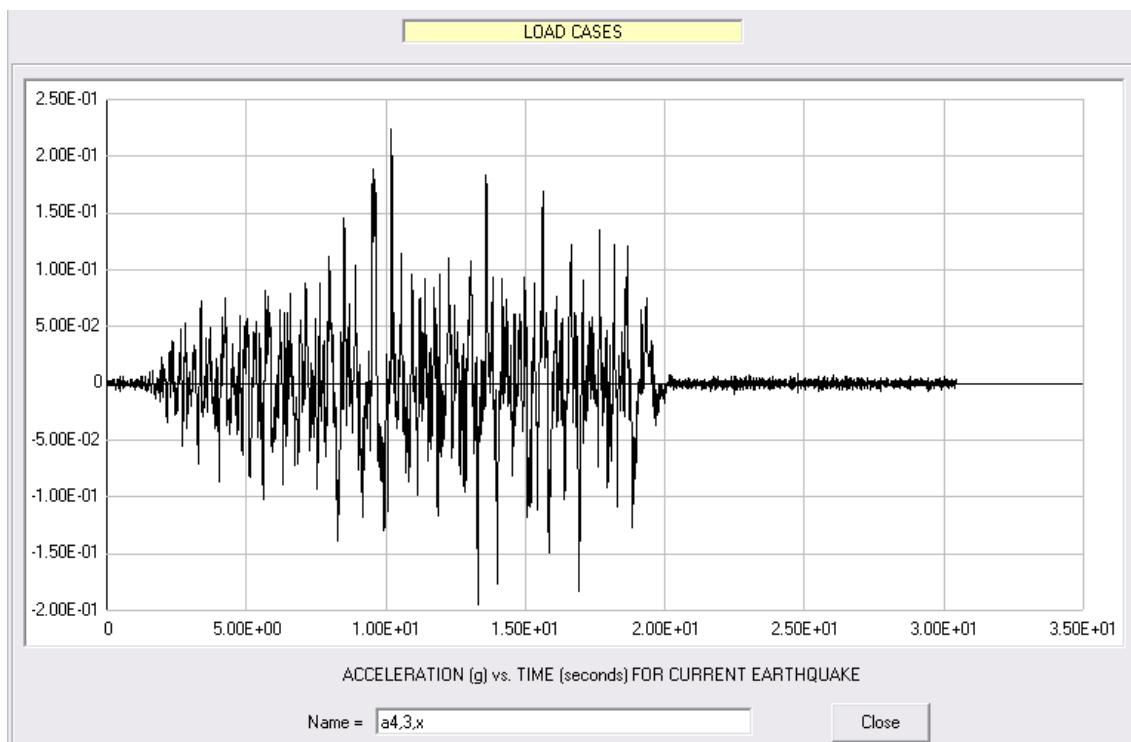


Figure 65 - A4 specimen test accelerogram (test number 3 – x direction) (program display).

It was chosen to the A4 model, the 0.22 g maximum acceleration model, that corresponds to the experimental test number 3 (see Figure 65).

These tests were chosen to study the models with a high and low PGA acceleration, being aware to the limits of the structure.

To define the analysis load case, it was chosen the dynamic earthquake category.

The tests were performed in the Q1 direction – down aisle direction – with a total time of 30.48 seconds, maximum of 200 steps and saving the results for each step – 0.01 seconds. The reference drift is the total one.

Chapter 4 - Accuracy of the numerical model

In this chapter a study of the accuracy of the numerical model is performed. To evaluate the overall accuracy of this model, it was necessary to do a study of the forces, the stiffness and energy dissipations. Due to the unawareness of information, it is studied just the displacements results and it is given the precision of the model in this area.

This chapter is sub-divided in the three specimens results.

4.1 - A1 specimen

These were the obtained results in the specimen A1. The results are sub-divided by floor.

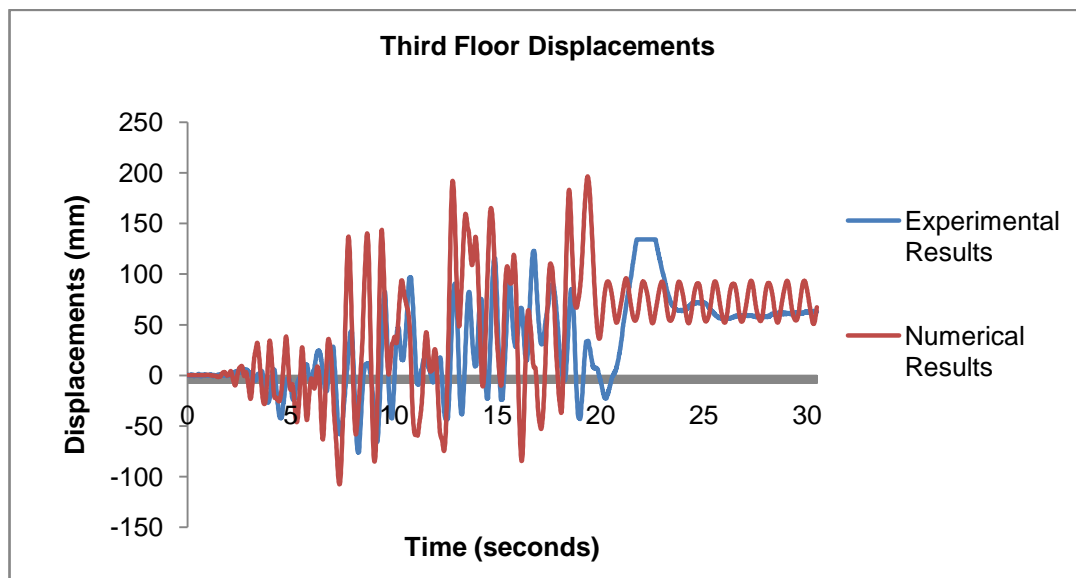


Figure 66 - A1 comparison between numerical and experimental displacement – third floor.

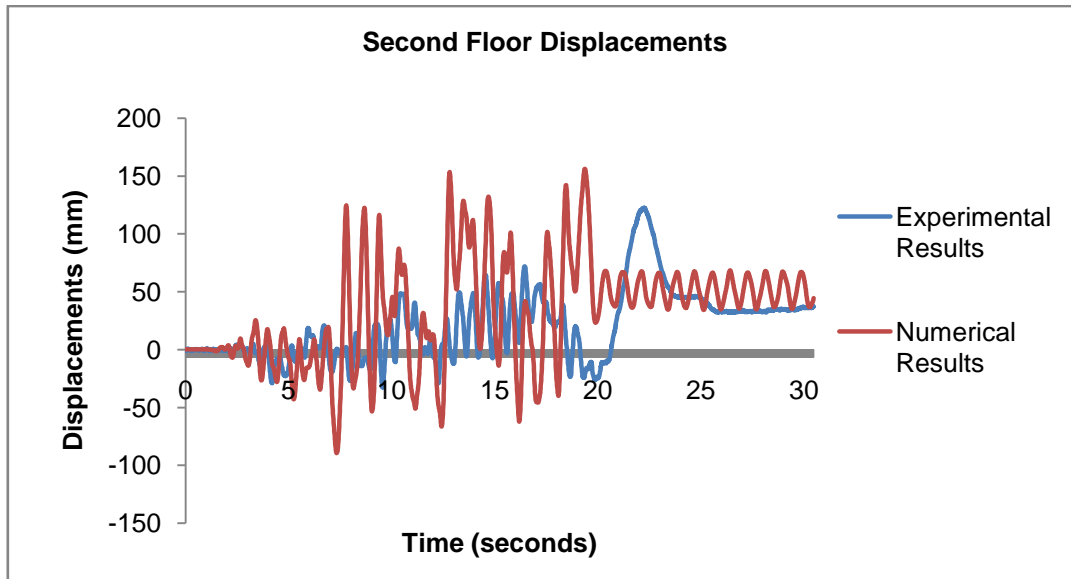


Figure 67 - A1 comparison between numerical and experimental displacement - second floor.

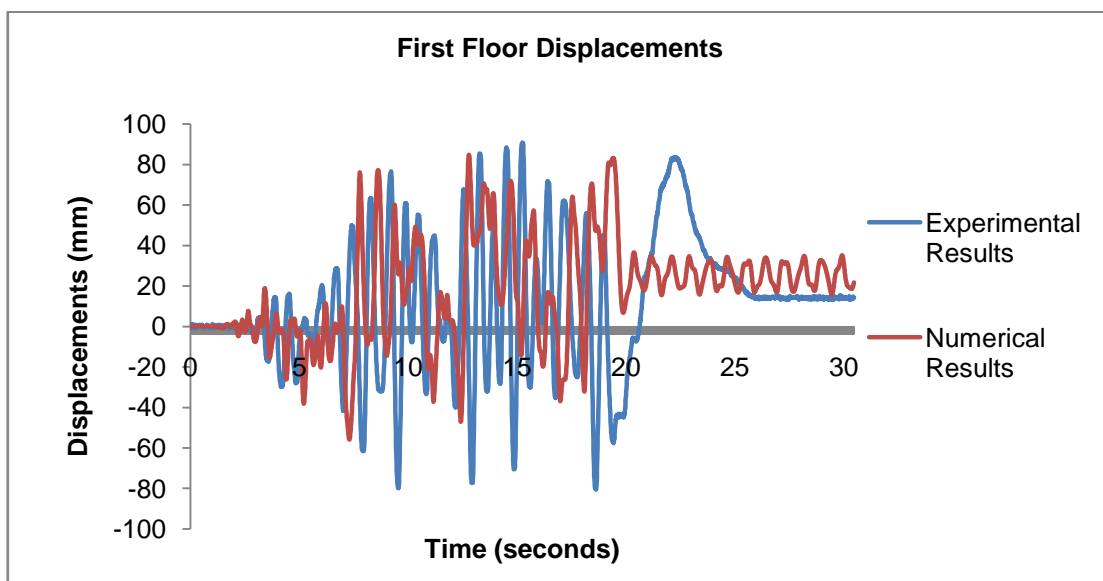


Figure 68 - A1 comparison between numerical and experimental displacement - first floor.

The graphics illustrate the displacements of the third, second and first floors.

Looking to the last ten seconds of the numerical results, it is notable that the structure has plastic deformations in this period. In comparison with the experimental results, it matches well.

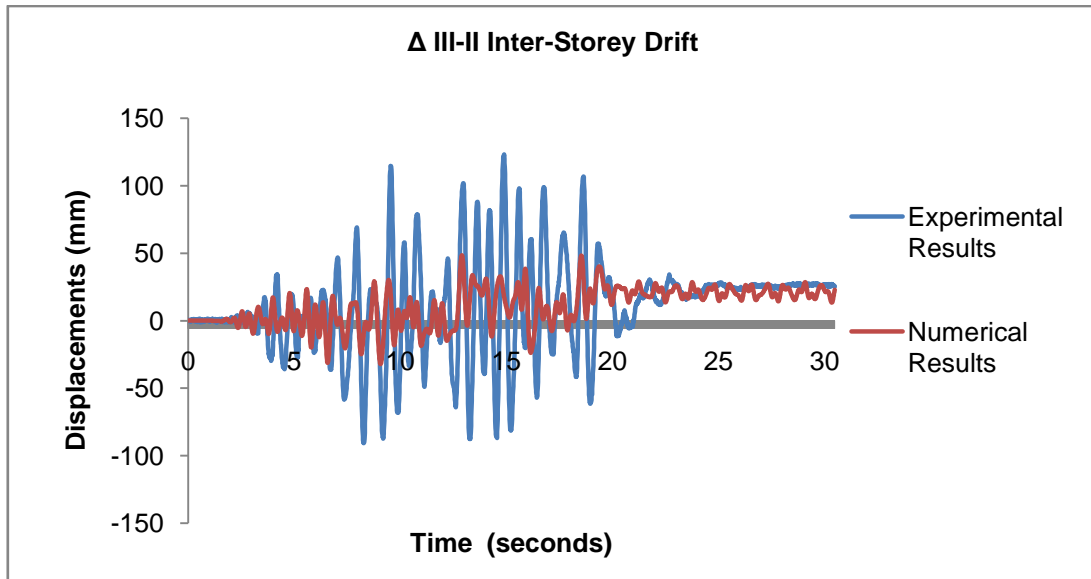


Figure 69 - Δ III-II Inter-Storey drift numerical/experimental comparison.

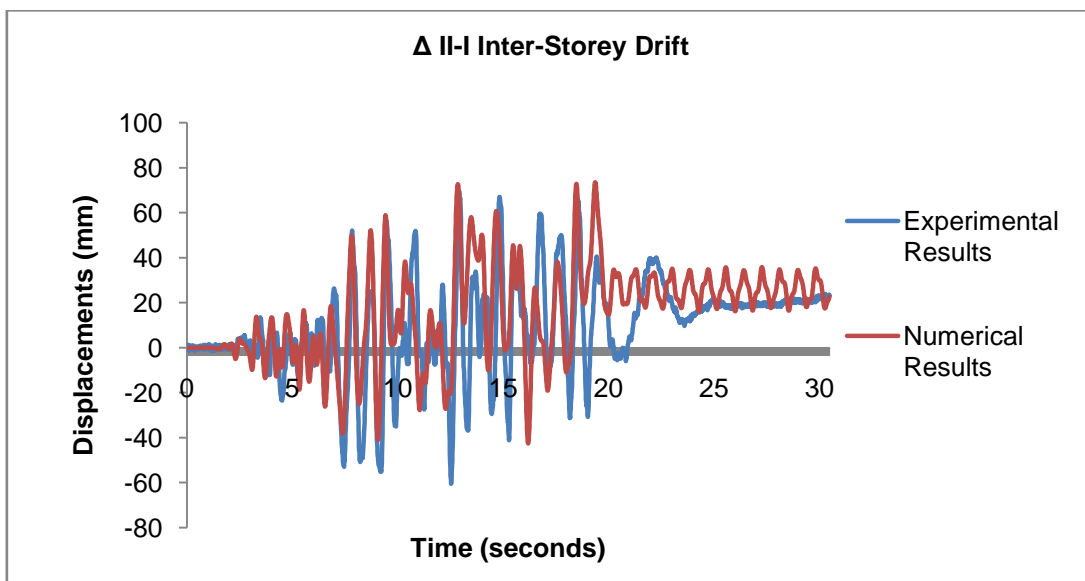


Figure 70 - Δ II-I Inter-Storey drift numerical/experimental comparison.

This graphics demonstrate the last levels inter-storey drifts.

In this structure the results are good. It is possible to see that the agreement and the values of the results of the first level match very well. The second and the third floor are less precise due to the maximum values are not matching so good; but the results remain acceptable.

This kind of structure was not the problematic one due to the fact of the pallets being fixed to the beam.

The drift graphics confirm the previous statement. As it is possible to observe, in the Δ II-I drift match very well, due to the good results of the first floor. The Δ III-II drift is not so good because the numerical model's displacements difference between the second and third floor is much smaller than the experimental model.

4.2 - A2 specimen

In this specimen the pallet is free to slide in the beam. Due to it, the results were highly affected in the last two floors.

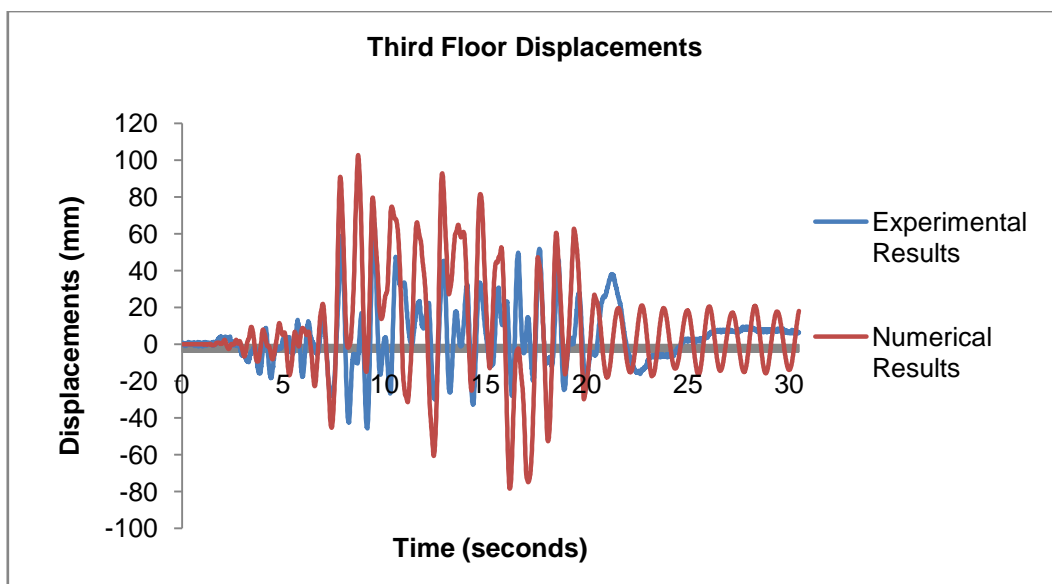


Figure 71 - A2 comparison between numerical and experimental displacement - third floor.

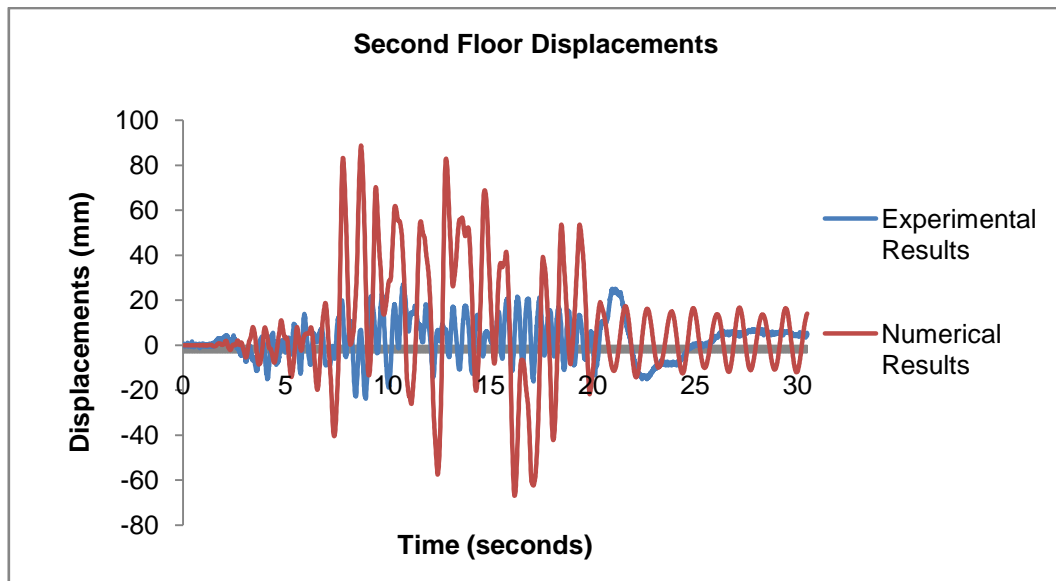


Figure 72 - A2 comparison between numerical and experimental displacements - second floor.

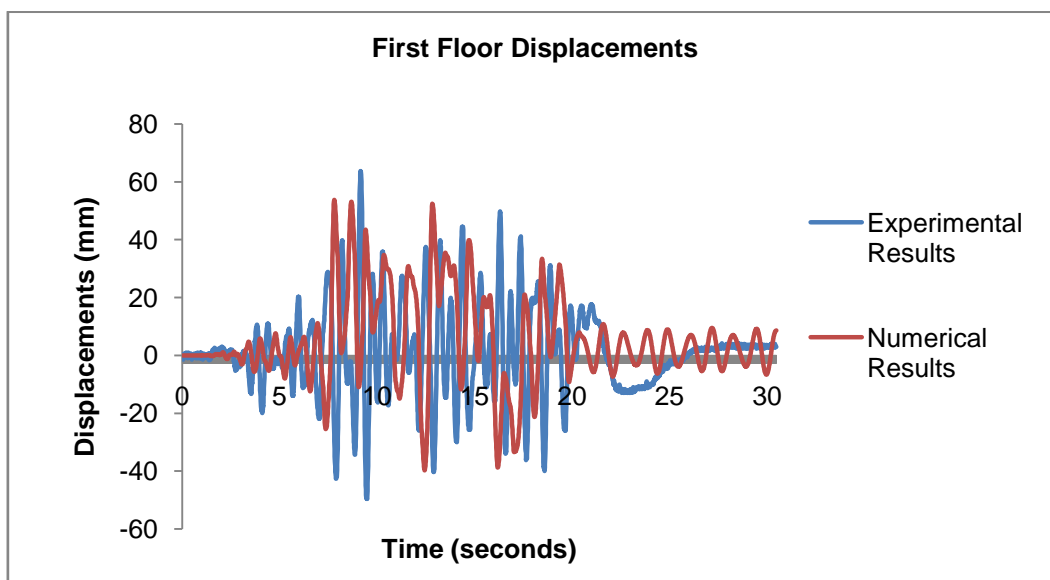


Figure 73 - A2 comparison between numerical and experimental displacements - first floor.

In this specimen, it is notable that a difference between the final state of the numerical and the experimental models exists. The numerical model has elastic deformations, as it is possible to observe. In the other hand, the experimental results, show plastic deformations in the structure between the 23 and the 30 seconds of the performed test.

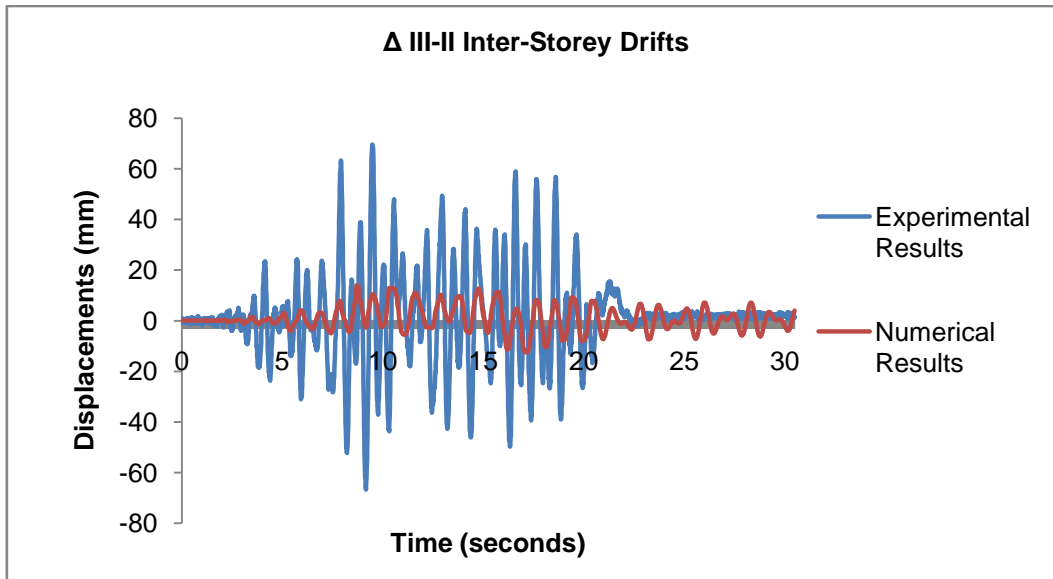


Figure 74 - Δ III-II Inter-Storey drift numerical/experimental comparison.

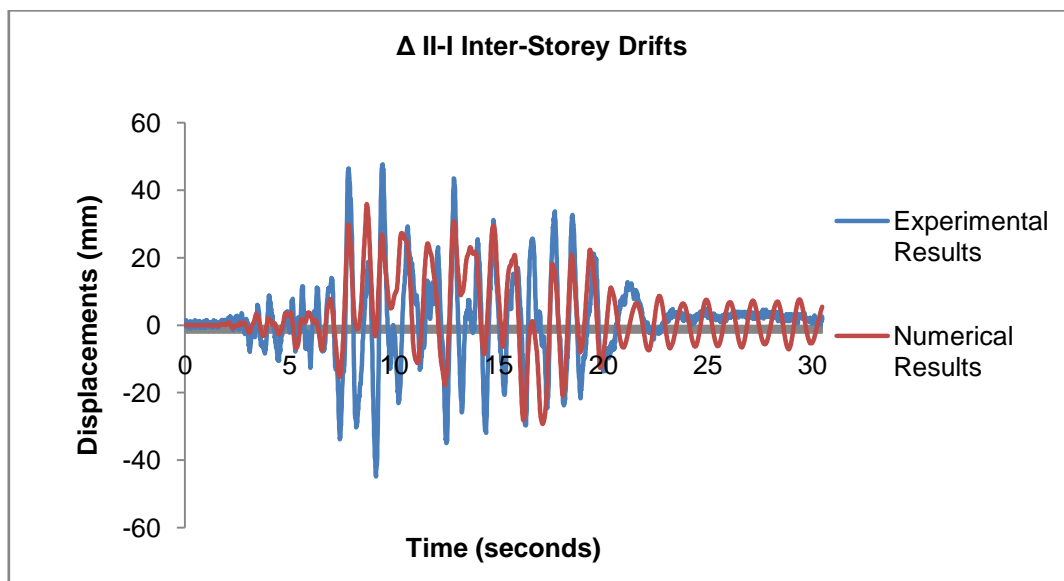


Figure 75 - Δ II-I Inter-Storey drift numerical/experimental comparison.

This graphics demonstrate the last levels inter-storey drifts.

Throughout a generically perspective, the results of this structure are not as good as the A1 specimen, but very acceptable. Once more, the first floor displacements contain the better results. Comparing to the experimental model, it has been obtained larger displacements in the second and third floor – their maximums do not match.

The drift results are also more precise in the first level than in the second one.

This was a complicated specimen, due to the calibration of the seismic device. To get these results it was needed to calibrate precisely the μ dynamic factor - calibrating directly the FU of the seismic device.

The μ dynamic factor is the friction factor. Friction is the tangential reaction force between two surfaces in contact. Physically these reaction forces are the results of many different mechanisms, which depend on contact geometry and topology, properties of the bulk and surface materials of the bodies, displacement and relative velocity of the bodies and presence of lubrication.

In dry sliding contacts between flat surfaces, friction can be modeled as elastic and plastic deformation forces of microscopically asperities in contact.

To calibrate the μ , it was used the expression,

$$F = \mu \times m \times a \quad (\text{eq.3})$$

The used mass rounds the 800 Kg (concrete blocks were used in the experimental tests) so, each seismic device carries a mass of 200 Kg, as it is possible to see in Figure 76. The acceleration is the gravity acceleration, and the used μ was 0.3. So, the defined FU was 0.6. This friction factor corresponds to a friction between the wood pallet and the beam.

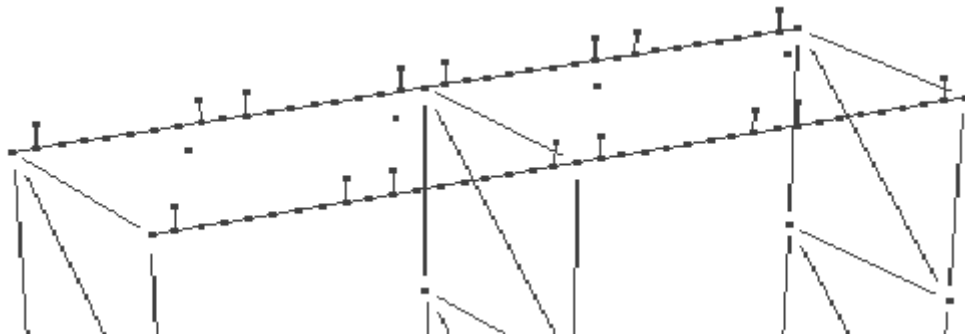


Figure 76 - Seismic device mass division (program display).

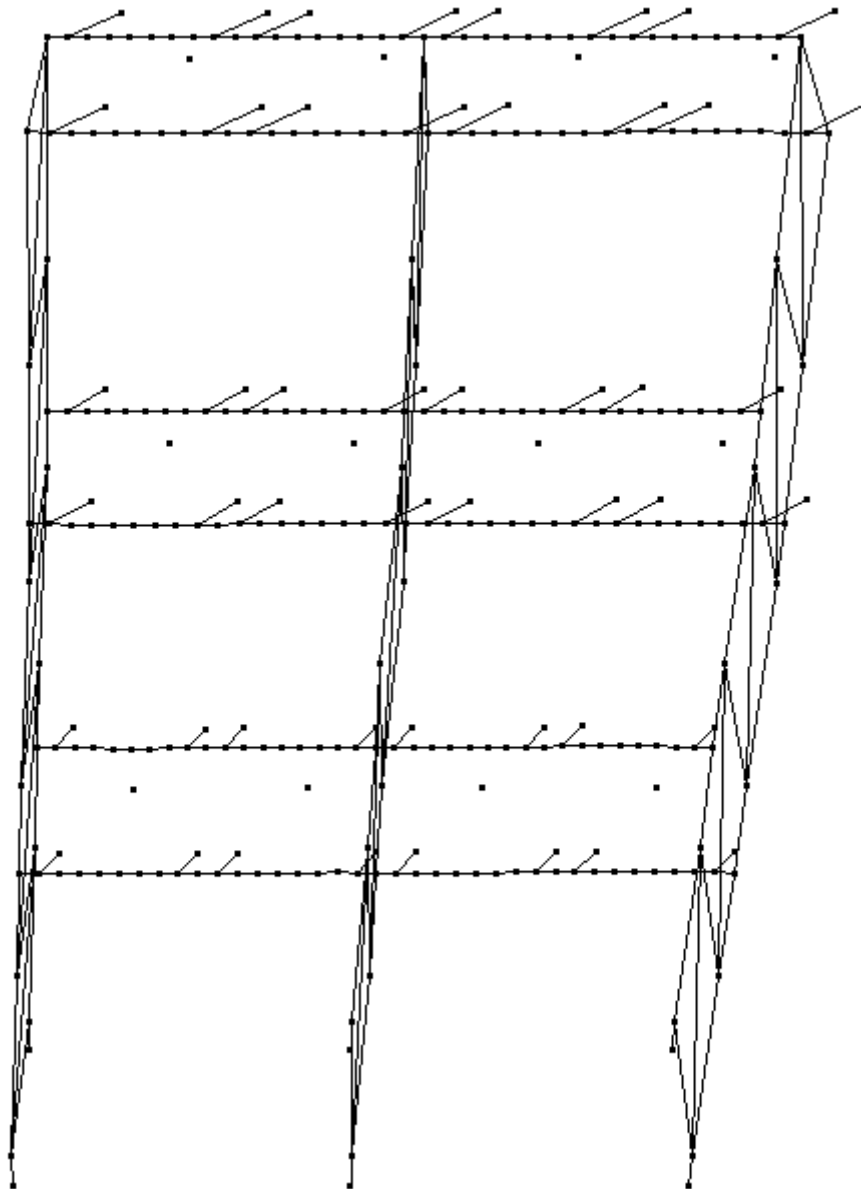


Figure 77 - First mode deformed shape (program display).

It is also curious to see the first mode deformed shape of the structure, noting that it is very similar to the experimental deformed shape (figure 27).

4.3 - A4 specimen

The A4 specimen was the most difficult model to analyze. This model was studied in the cross-aisle direction.

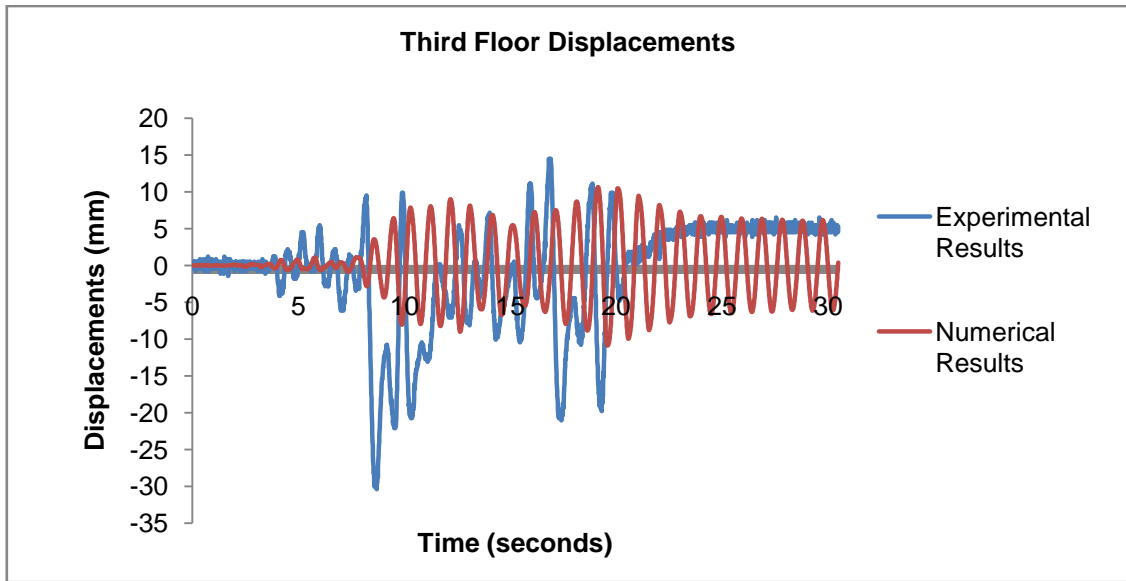


Figure 78 - A4 comparison between numerical and experimental displacements - third floor.

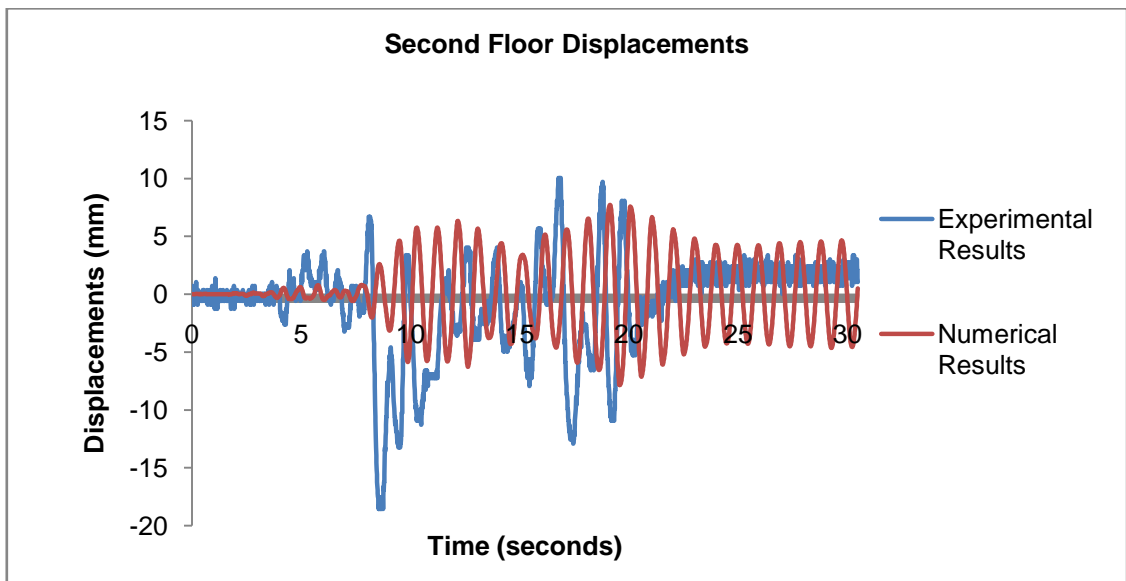


Figure 79 - A4 comparison between numerical and experimental displacements - second floor.

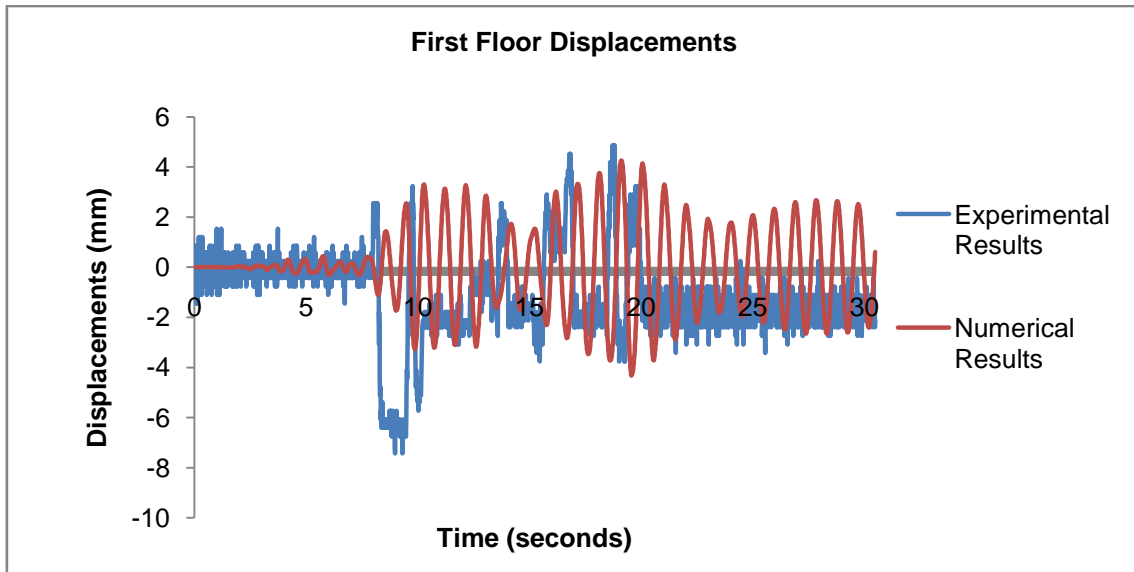


Figure 80 - A4 comparison between numerical and experimental displacements - first floor.

As it is happening in the A2 specimen, the numerical model is having elastic deformations. In the other hand, the experimental model finishes the test with plastic deformations.

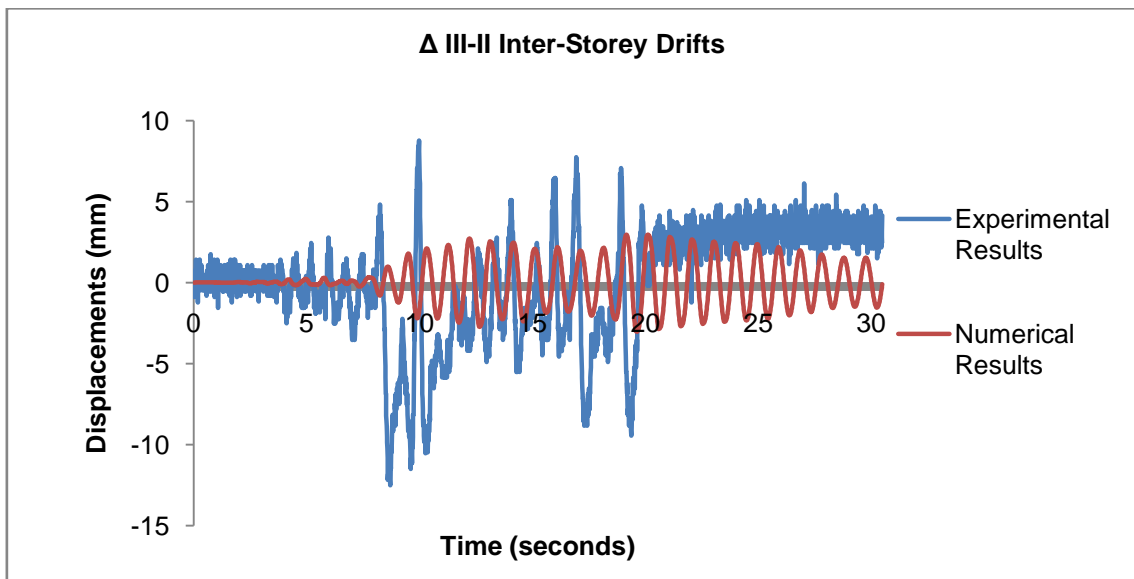


Figure 81 - Δ III-II Inter-Storey drift numerical/experimental comparison.

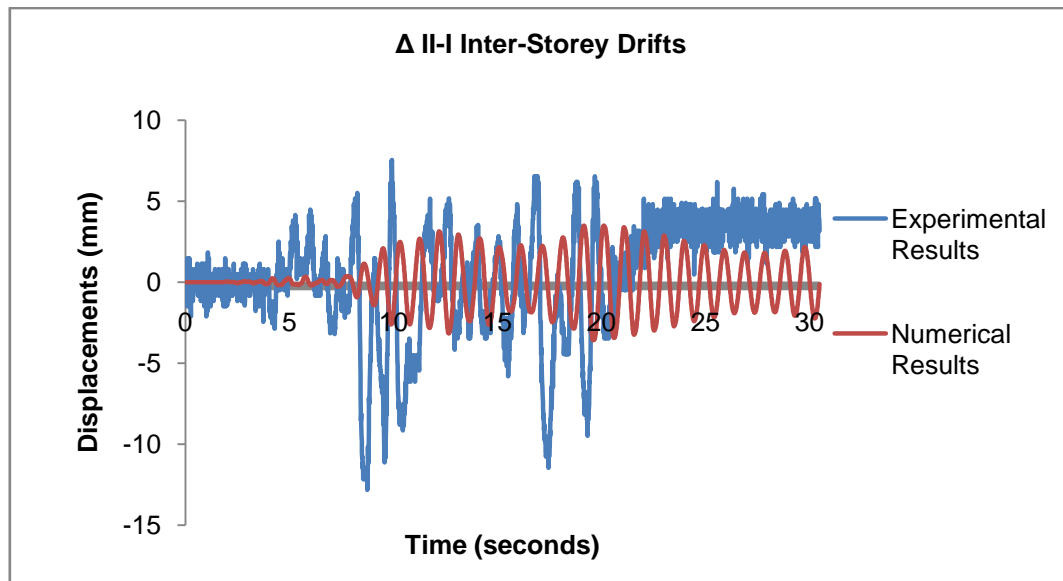


Figure 82 - Δ II-I Inter-Storey drift numerical/experimental comparison.

This graphics illustrate the last levels inter-storey drifts.

The values of the three floors generally match well. The higher values of the experimental model do not match. The agreement of this specimen is not the best. Consequently the drift graphics are not the most accurate.

To improve the results, the seismic device was defined with a higher FU – 1.2 KN and the stiffness of the beam-to-column connection, in the cross aisle direction, were decreased to 1/10. The reason to this is the fact of the pallet rack's rigidity being much higher in the down aisle direction than in the cross aisle direction.

All these factors are being considered to get the best possible results.

The results of this specimen are acceptable, taking in consideration all the experimental failures (analyzed in the chapter 2) and all the missing information about the connectors in this direction.

It is important refer that the stiffness of the connections between the uprights and the bracing members of the transversal frames is not known, and was simulated as a hinge. This is also probably the cause for the discrepancies between numerical and experimental results. They are due to difficulty in calibration of the stiffness of the transversal frames.

4.4 - Conclusions

The A1 specimen results were satisfactory, taking in consideration that this was the simplest structure, due to the analysis direction – down-aisle - and the fixed pallet-beam relation.

The A2 specimen results were very acceptable, but numerically speaking it was the worst of the three. The sliding pallet had an important influence and consequently the seismic device definition.

The A4 specimen was, in the beginning, the problematic specimen. The unawareness of the beam-to-upright connection properties was determinant. But, taking it into account, the results were very good, considering that was the unique specimen that had the numerical results under the experimental ones, that transmits confidence to this numerical study.

Generally, the results were satisfactory, and it is conclusive that the model had a good accuracy in the displacements area. Forces, stiffness and energy dissipations are fundamental to the global accuracy of the model. It is a possibility of a future study in this area.

Chapter 5 - Conclusions

5.1 - General conclusions

The sliding of the pallets on the racks and their consequent fall represents a serviceability limit state i.e. a situation that might occur during a seismic event also in the case of a well designed storage rack.

The seismic action in this kind of structures is a topic of study that, nowadays, is in constant development.

This dissertation developed the study of the racking system in helping to avoid human and economical consequences, throughout the understanding of the behavior of the pallet sliding in the racks.

The development of a numerical model was leaded, with all the properties of the experimental specimens. An accuracy of this model was verified by the comparison of the displacements of each model.

Several tries and simulations were done in this study in order to get the best possible results.

Other problem was the simulation of the pallet and its friction with the beam. This problem was solved, by the study of the program seismic device.

It is important to mention that a good accuracy of the model requires a study of the forces, stiffness, energy dissipations and displacements. In this dissertation only the displacements results were studied due to the available information.

The obtained results were acceptable, taking in consideration all the factors that were mentioned before – unawareness of some devices characteristics.

The initial aims of this work were accomplished. The model could be calibrated and its results improved.

In the future, the study of the forces, stiffness and energy dissipations of the model, allowed that the study could be performed by computer software, dismissing the experimental projects, giving a good economical and scientific improvement to this study.

With this work, the numerical study of the pallet racking systems is improved. Some ideas to a future possible study are given in the next sub-chapter.

5.2 - Future development

Other studies can be done in the area of the pallet sliding. The moving of the masses is an important factor in the pallet racking system.

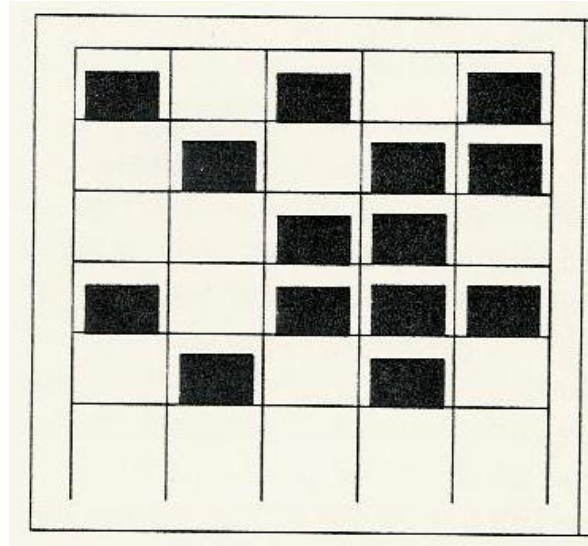


Figure 83 - Rack study possibility.

Other possibility is studying the kind of loads that are used to test the structure, i.e., this study was done with concrete blocks. It is considered to be an accurate procedure to test the behavior of the structure with the pallet loaded with liquids, motorbikes or other kind of merchandise.

It is also raised the possibility of performing a study of a different structure configuration, with the objective of analyzing the consequences of the redistribution of the loads and the increasing of the number of bays or even of the number of the stories. Playing with the masses, it is possible to study the effect of the loads, taking always in consideration the kind of pallet, the kind of material that is stored, the acceleration and frequency of the shaking-table test, as it was seen before. (See figure 84).

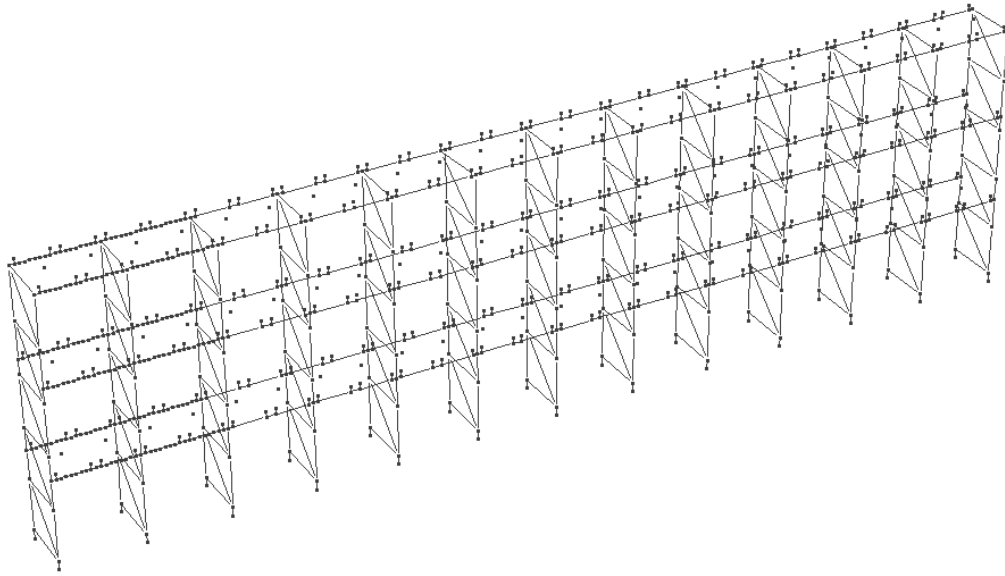


Figure 84 - Other configuration (program display).

References

A.S. 4084 (1993), *Steel Storage Racking*, Australian Standards

Agatino, M.R., Bernuzzi C. and Castiglioni C.A. (2001), Joints under cyclic reversal loading in steel storage pallet racks, *Proc. of XVIII Conference C.T.A., Venezia*, September 2001, pp. 105-114.

ATC-3 (1978), *Tentative Provisions for the Development of Seismic Regulations for Buildings*. Applied Technology Council, Redwood City, CA.

Baldassino, N. and Bernuzzi C. (2000), Analysis and Behaviour of Steel storage Pallet Racks, *Thin-Walled Structures*,. 37 (4), 277-304.

Baldassino N. and Zandonini R. (2001), Numerical and Experimental Analysis of Base-plate Connections of Steel Storage Pallet Racks, *Proc. of XVIII Conference C.T.A., Venezia*, 127-136

Castiglioni C.A., Panzeri N, Brescianini J.C. and Carydis P. (2003) Shaking Table Tests on Steel Pallet Racks, *Proceedings of the Conference on Behaviour of Steel Structures in Seismic Areas-Stessa* 2003, Naples, Italy, 775-781.

Castiglioni C.A. (2003). Dynamic Tests on Steel Pallet Racks, *Costruzioni Metalliche*, **55**(3), 35-44

Chen C.K., R.E. Scholl and J.A. Blume (1980a), Seismic Study of Industrial Storage Racks, *Report prepared for the National Science Foundation and for the Rack Manufacturers Institute and Automated Storage and Retrieval Systems (sections of the Material Handling Institute)*, John A. Blume & Associates, San Francisco, CA.

Chen C.K., R.E. Scholl and J.A. Blume (1980b) Earthquake Simulation Tests of Industrial Steel Storage Racks. *Proceedings of the Seventh World Conference on Earthquake Engineering*, Istanbul, Turkey, 379-386.

CSI Computers and Structures, *Perform Components and Elements*, version 4, August 2006

CSI Computers and Structures, *Perform User Guide*, version 4, August 2006

FEM 10.2.02 (2001) a, *The Design of Static Steel Pallet Racks*, Federation Europeen de la Manutention, Vers. 1.02

FEM 10.2.04 (2001) b, *Guidelines fot the safe use of static steel racking and shelving*, Federation Europeen de la Manutention, Vers. 1.02

FEM 10.2.08 (2005), *The Seismic Design of Static Steel Pallet Racks*, Federation Europeen de la Manutention, final draft, December 2005.

FEMA (2005), *Seismic Considerations for Steel Storage Racks Located in Areas Accessible to the Public, FEMA 460*, September 2005

Filiatrault A., Bachman R.E., Mahoney M.G. (2006), Performance-Based Seismic Design of Pallet-Type Steel Storage Racks, *Earthquake Spectra*, 22 (1), 47–64

John A. Blume & Associates (1973), *Seismic Investigation of Steel Industrial Storage Racks*, Report prepared for the Rack Manufacturer's Institute, San Francisco, CA

John A. Blume & Associates (1974), *Seismic Design Examples of Industrial Storage Racks*, Report prepared for the Rack Manufacturer's Institute, San Francisco, CA.

John A. Blume & Associates (1987), *Application of Eccentric Bracing to Rack Structures*, Report prepared for the Rack Manufacturer's Institute, San Francisco, CA.

RMI. (2002) a, *Specification for the design testing and utilization of industrial steel storage racks*, Rack Manufacturers Institute, Charlotte, NC., 2002 edition

RMI. (2002) b, *Commentary to Specification for the design testing and utilization of industrial steel storage racks*, Rack Manufacturers Institute, Charlotte NC.

SEISRACKS (2007), *Storage Racks In Seismic Areas (SEISRACKS), Research Programme of the Research Fund for Coal and Steel RTD*, Final Report, May 2007

www.csiberkeley.com